CONVERSION OF SUGARCANE BAGASSE INTO CARBOXYMETHYL CELLULOSE

FEZOKUHLE MFUNDO MAKHANYA

Submitted in fulfillment of the requirement for the degree of

Master of Applied Sciences in Chemistry

Faculty of Applied Sciences at the Durban University of Technology, Chemistry Department, Durban, South Africa

November 2020

To my mother Nozipho Faith Makhanya, sister

Thulile Charmaine Makhanya and late friend Mfundo Hopewell 'Bling' Mseleku

PREFACE

I hereby declare that this research is the result of my own investigation, which has not been already submitted in substance for any degree and is not being submitted in contention for any degree.

Student: Date

Fezokuhle Mfundo Makhanya

Supervisor: Date:

Prof. N. Deenadayalu

ACKNOWLEDGEMENTS

I am exceptionally thankful to God for the strength and the ability to overcome all obstacles that have been stumbling blocks in my time as a student, a special thanks goes to the following:

My family for believing in me and the constant encouragement during this period, when obstacles were there, they helped me overcome them.

My Supervisor Prof. N. Deenadayalu for giving me an opportunity to pursue my studies and guiding me throughout my study.

Durban University of Technology for the opportunity and lessons it has taught me as a person and especially as a first-time researcher.

Mangosuthu University of Technology, Chemistry Department, for laying the foundation to my education and skills in the laboratory and for the extra assistance with my experimental work and characterization.

DUT Research Office and NRF for funding my studies.

UKZN, Westville Campus's Electron Microscopy unit for all SEM and TEM images.

University of Johannesburg, Department of Chemistry for all XRD data.

ABSTRACT

The process of converting sugarcane into sugar has a high percentage of dry residue that remains after the juice has been extracted, the dry residue is referred to as sugarcane bagasse (SCB). The focus of this study has been on using sugarcane bagasse to extract cellulose from the matrix and converting it into carboxymethylcellulose (CMC). This has been achieved via a two-step synthesis process. Mill run sugarcane bagasse was used as received and was pre-treated using NaOH for the purpose of extracting cellulose from the sugarcane bagasse. The extractant was refluxed separately using two different nitric acid (HNO_3) concentrations namely 8 M (cellulose sample 1) and 4 M (cellulose sample 2) in 20 % (v/v) ethanol to obtain cellulose. The extracted cellulose was obtained in yields of 37 % and 40 % for the 8 M and 4 M HNO_3 concentrations. The extracted cellulose was converted into carboxymethyl cellulose. The synthesis was done by a carboxymethylation reaction where the cellulose was reacted with different NaOH concentrations (m/v %) namely 20 %, 25 % and 30 %. The CMC yield (m/m %) %) was 120 %, 125 % and 140 %, respectively at the different NaOH concentrations (20 %, 25 % and 30 %). The higher concentration of NaOH facilitates greater carboxymethylation.

The extracted cellulose, synthesised CMC and the commercial samples of cellulose and CMC were characterized using Fourier transform infra-red spectroscopy (FTIR), transmission electron microscopy (TEM), scanning electron microscopy (SEM), thermogravimetric analysis (TGA), differential scanning calorimetry (DSC) and X-ray diffraction (XRD) techniques.

The FTIR spectrum of the commercial cellulose exhibited peaks at 3334 cm^{-1}, this peak was characteristic of the –OH stretching vibration. Cellulose samples 1 and 2 showed peaks at 3306 cm^{-1} and 3331 cm^{-1}, respectively for the similar vibration.

The commercial CMC sample showed FTIR peaks at 1400 cm^{-1} and 1600 cm^{-1}, which corresponded to the carboxymethyl substituent. The extracted CMC from sugarcane bagasse showed the similar peaks at 1439 and 1631 cm^{-1}, respectively.

The TEM and SEM images for all cellulose samples showed that the spherical shape of commercial and extracted cellulose were similar in length and width, the extracted cellulose samples appear

to be longer in length compared to the commercial cellulose. The TEM results for all cellulose samples appear to be similar from the images. Both commercial and extracted CMC sample TEM images showed highly dispersed and crystalline particles that are consistent with those observed for carboxymethylated cellulose. The CMC particles observed appear to be dark spots that are spherical. SEM images for CMC samples showed a contrast to cellulose samples, the surface was smoother in appearance that correlated strongly with CMC SEM images observed in literature and the commercial sample.

XRD diffraction patterns showed two significant peaks at 2Θ = 15° and 22.5° that confirmed the presence of cellulose I and cellulose II, respectively, in both the commercial and extracted cellulose samples. Both commercial and synthesised CMC samples had a single peak at approximately 2Θ = 20°, characteristic cellulose peaks are no longer visible on the diffractograms.

The TGA scans showed that the cellulose sample degraded similarly to the commercial cellulose sample. The TGA scans of synthesised CMC and the commercial CMC samples showed similar degradation patterns.

DSC scans also showed similar trends for the commercial and synthesised CMC samples. The DSC curves showed that all samples had two major peaks: a small peak for moisture loss between 50 °C - 90 °C and a more significant peak at approximately 350 °C due to decarboxylation and CO_2 bond breakage.

The degree of substitution (DS) for the commercial CMC sample was 0.420 and for the extracted CMC samples there was an increase in DS to 0.357, 0.366 and 0.420 which correlated with an increase in NaOH concentration (20 %, 25 % and 30 % (w/v)), respectively.

Characterization for this study confirmed the successful delignification of sugarcane bagasse as confirmed by the similar properties of commercial cellulose. Furthermore, the carboxymethylation was successfully achieved at various NaOH concentrations. The study gave insight on how each of the parameters optimized affected the production of the bio-derived cellulose and CMCs. A comparision of the commercial cellulose and CMCs with the bio-derived cellulose and CMCs showed that they were successfully extracted and synthesised, respectively.

Contents

List of Tables

List of Figures

Symbols and Abbreviations

SCB	- Sugarcane bagasse
CMC	- Carboxymethyl cellulose
DP	- Degree of polymerization
DS	-Degree of substitution
2Ɵ	- 2 Theta degree
cm^{-1}	- wavenumber
CMC	- carboxymethyl cellulose
MPa	- Mega Pascals
LM	- Lignocellulosic material
MCA	- Monochloroacetic acid
SCB	- Sugarcane bagasse
VS	- Vine stem
MCC	- Microcrystalline cellulose

CHAPTER ONE

INTRODUCTION

1.1 Background

The current primary industrial objective is to source numerous raw materials for chemical use as starting materials in many polymer industry reactions. The materials should ideally be used in a sustainable manner (Duncan, 2011: Rhim et al. 2013). Various studies have been conducted in this regard and they all show that potential use of biomass is a great and viable option for production of platform chemicals used in industry. Biomass sources are now currently being used in many processes as a starting material (Moncada et al. 2014). It has also been shown that fibre, and a wide range of biomolecules can be obtained from biomass using a biorefinery approach (Moncada et al. 2014). The first-generation sources of biomass were mainly edible crops used mainly for food or agricultural use. The second generation however, are mainly comprised of lignocellulosic materials (LMs) and these are namely composed of cellulose, hemicellulose and a high lignin content. These materials are produced through varied extractions or transformation stages such as seeding, cropping, harvesting as well as processing (Rincón et al. 2014). The second generation of biomass were designed in such a way that they did not directly compete with food production which is highly advantageous. Lignocellulosic materials are found abundantly which is also advantageous, they however have a main drawback when it comes to their use as it is difficult to extract cellulose from the matrix. This refers to the ability of these lignocellulosic plant material to resist microbial attack this makes it difficult to easily isolate the components and thus pre-treatment methods are necessary and play a vital role in production (Himmel et al. 2007). Industrially cellulose from wood, agricultural residue and paper mills have been converted into sugars by pre-treatment of feeds with acids or cellulolytic enzymes.

1.2 Lignocellulosic materials (LMs)

Bio-based materials from digestion of various lignocellulosic materials has shown and strongly continues to show that it is a great alternative to fossil fuels. Globally 1368 million tons per year of the world's biomass is attributed to LMs (Limeyana and Ricke et al. 2012). The use of LMs as feedstocks such as agricultural waste has provided a valuable alternative from edible food crops which were being used as liquid fuels such as ethanol and butanol (Perlack et al. 2005). The main advantages of these materials are they are cheap and abundant, and some are even non-food as mentioned but are rich in lignocellulose (Limayem and Ricke et al. 2012). LMs are made up of three main subcomponents: semi-crystalline polysaccharide cellulose, the multicomponent polysaccharide hemicellulose and the amorphous polymer lignin (Perlack et al. 2005). Sugarcane bagasse, the residue after sugar production is a promising bioresource.

1.3 Carboxymethyl cellulose (CMC)

1.3.1 Introduction

Due to CMCs outstanding physical properties such as: biocompatibility, biodegradability and renewability as a polysaccharide it can be used in the production of high value-added products (Cheng, 1999: Kulicke et al. 2006). CMC is a polysaccharide product that is a biodegradable polymer which is highly demanded on the market (Dolbow et al. 2005). Presently there are various applications for CMC such as varnishes, dyes, textile sizing, and as a thickener in many household and industrial products (Gupta et al. 2013). There are also varying grades of commercial CMC with the technical grade being used in detergents (Hader et al. 1952) and an intermediate grade which is not as purified being used in the paper industry (Padam et al. 2015). To utilize CMCs in various industries it is important that the cellulose be converted into its derivatives and CMC is a product of such processes. CMC is the common derivative of cellulose which is made up of a long chain of linear anionic water-soluble bonds. A pure commercial CMC sample is an off-white coloured, tasteless salt that is free flowing (Satti et al. 2015).

1.4 Characterization of cellulose and synthesis of CMC

For this project cellulose is extracted from sugarcane bagasse (SCB) and used to synthesise CMC. Thereafter the process involved the conversion of cellulose in aqueous NaOH and an organic solvent (typically ethanol or isopropanol) with monochloroacetic acetic acid (Heinze and Pfeiffer et al. 1999). Most work that has been done previously has focussed on the mechanical properties of CMC obtained from sugarcane bagasse.

In this work the material properties that were characterized included the change in surface morphology from cellulose to CMC, particle size and crystallinity changes were also briefly analysed. These were done using analytical techniques such as Powder X-Ray Diffraction (PXRD), Scanning Electron Microscopy (SEM) and Transmission Electron Microscopy (TEM). These characterizations were to be compared to that of commercial grade samples and those observed in literature. The chemical decompositions of the material were also investigated by means of thermal studies mainly Thermogravimetric Analysis (TGA) and Differential Scanning Calorimetry (DSC).

This study is unique because cellulose is extracted from sugarcane bagasse (SCB) and used to synthesise CMCs. Many researchers have used commercial cellulose to synthesise CMCs.

1.5 Scope of Dissertation:

The dissertation is divided into 5 chapters with information as follows:

Chapter One: **Introduction**- Highlights the main topics; Background information of the study, the concept of lignocellulosic materials (LM's), carboxymethyl cellulose (CMC) and the characterization and synthesis of CMC from extracted cellulose.

Chapter Two: **Literature Review**-covers the following - Applications of sugarcane bagasse; Paper industry; Intermediate product or raw material; Cellulose pre-treatment methods; Types of pre-treatment methods; Review of applications of sugarcane bagasse; review of cellulose pre-treatment methods. Also a review of mechanical applications of cellulose, cellulose derivatives such as carboxymethyl cellulose including their properties such as solubility degree of substitution (DS) and morphology: factors that impact on viscosity, synthesis of CMC's and their applications including pharmaceuticals, oil drilling, ceramics, insecticides, paper, tobacco and mining.

Chapter Three: Materials and Experimental discusses materials and experimental procedures detailing the extraction of cellulose from sugarcane bagasse process, the yield of cellulose obtained from extraction and the synthesis of CMC from the extracted cellulose. Characterization techniques for cellulose and CMC were done such as the degree of substitution (DS) which was done only for CMC using titrimetric techniques. The fundamental concepts of characterization techniques such as; Attenuated total reflectance (ATR) - Fourier Transform Infra-Red Spectroscopy (FTIR), Powder X-ray Diffraction (PXRD), Thermal analysis and Electron Microscopy.

Chapter Four: **Results and Discussion** covering the cellulose extraction from waste biomass; the impact of nitric acid concentration on yield, CMC synthesis. Characterization results discussed for extracted cellulose and synthesized CMC.

Chapter Five: **Conclusion** is a summary of the obtained results.

References - the list of references are given at the end of the dissertation.

CHAPTER TWO

LITERATURE REVIEW

2.1 Introduction

Globally sugarcane bagasse (SCB) is known for being one of the most promising agricultural resource of our generation for sourcing biomass energy and bio-based industrial applications (Zafar et al. 2015). It can produce two types of biomass which are cane trash and sugarcane bagasse. Cane trash which is defined as the field residue remaining after the cane stalk is harvested, while sugarcane bagasse is the fibrous residue that remains after milling of the cane for sugar production. Most sugarcane bagasse consists of cellulose, hemicellulose and lignin, it may sometimes contain wax and minerals (Zafar et al. 2015). **Table 2.1** shows the range of a typical sugarcane bagasse composition.

Table 2.1.: Typical composition of sugarcane bagasse (Katyal et al. 2003).

Component	**Percentage Composition (%)**
Cellulose	26.6-54.3
Hemicellulose	22.3-29.7
Lignin	14.3-24
Moisture	40-50
Soluble solids	2-6

The sugarcane bagasse used in this study had a chemical composition of 43 % cellulose, 25 % hemicellulose, 23 % total lignin and the rest attributed to extractives (Chambon et al. 2018). Cellulose is made up of the glucose monomer which has a crystalline structure. Hemicellulose is an amorphous polymer usually composed of xylose, galactose, arabinose, glucose and mannose. The remainder is lignin which is an aromatic component of bagasse, trace amounts of wax and other soluble solids may be found (Sun and Sun et al. 2004).

2.2 Applications of sugarcane bagasse

In the sugar industries sugarcane bagasse is usually combusted in furnaces to provide steam for power generation for their own use. The US energy development sector that deals with the different uses for sugarcane bagasse have shown that it can be a viable feedstock in bioethanol production (Marin et al. 2016). SCB is used as a raw material in the paper industry and in agricultural industries as a feedstock for cattle. For every 1 ton of sugarcane crushed, a sugar factory can produce up to 300 kilograms of wet sugarcane bagasse with over 500 million tons produced globally (Bezzera and Ragauskas et al. 2016).

2.2.1 Paper industry

Sugarcane bagasse is also used in the production of pulp and paper. The applications thereafter are varied but SCB accounts for approximately 2-5% of global pulp and paper production that is a high revenue earner for the sugarcane industry (Rainey and Covey et al. 2016).”There are currently over 30 countries globally that use sugarcane bagasse for their paper manufacturing processes. The paper industry is said to be a steadily growing one with projections estimating a peak in demand in 2035 and much of the demand will come from packaging and tissue sectors (Wilson et al. 2013). Emerging economies are directly linked with these projects into sugarcane bagasse and its usage in the pulp and paper industries it is estimated that in the pulp and paper industry, bagasse will become more important as a paper feedstock (Rao et al. 1997).

2.2.2 Intermediate product or raw material

SCB is used as a direct and indirect starting material in industry to manufacture many other household materials and chemicals (Ponce et al. 1983) these materials include:

waxes, flavourants, sweeteners, anti-cholesterol drugs, furans, furan derivatives, cosmetics, emulsifiers, insecticides, preservatives and fuel oils. Economically some uses of sugarcane bagasse yield a higher return than that of mainstream sugar production (Bilal et al. 2017). As a result, many valuable production streams have developed from sugarcane bagasse that over time it will no longer be regarded as a by-product (Bilal et al. 2017). This also raises interest as researchers are extensively finding new and improved ways to utilize sugarcane bagasse (Banda et al. 2002).

2.3 Cellulose

Cellulose is the most abundant naturally available lignocellulosic material, it is known for its remarkable physical and chemical properties that have been highly utilized over the past few centuries industrially. Cellulose derivatives have also been highly sought after with multiple applications in various sectors (Klemm, 2005: de Menezes et al. 2009). Cellulose has the chemical formula $C_6H_{10}O_5$ and an elemental study showed that the chemical configuration of cellulose was 44.4% C and 6.2 % H (Krassig and Schurz, 1986: Koh et al. 2013). The molecular structure of a cellulose unit can be described as: a linear polymer, with a D-anhydroglucopyranose monomer. This unit is linked together by β-(1,4)-glycosidic bonds that form between carbon 1 (C1) and carbon 4 (C4). In their solid-state cellulose units are rotated 180 ° with respect to each other due to the limitations imposed by the β-linkage. Each unit of cellulose that forms part of the anhydroglucose unit has three hydroxyl groups (R-OH) on the carbon 2,3 and 6 positions, respectively. The hydroxyl group found on carbon 1 on both ends of the long chain of the molecule has an aldehyde group (C=O). This aldehyde is where the reducing properties are found. Each carbon has an alcohol borne hydroxyl group constituent and this gives it the ability to be a non-reducing end of the chain. **Figure 2.1** shows the chemical structure of the above-mentioned cellulose unit.

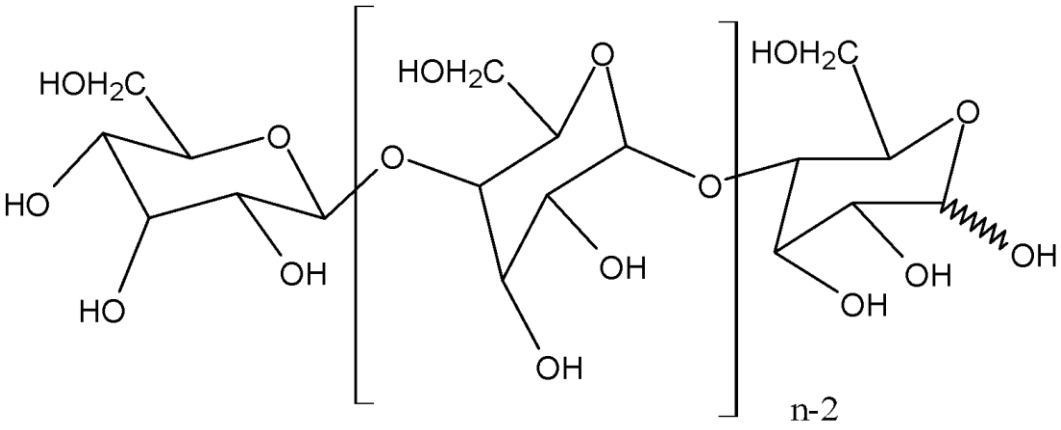

Figure 2.1: Cellulose structure (Michelin et al. 2014).

In plant material cellulose is found in an amorphous state and rather difficult to confine to a definite shape or form. It is also found in a crystalline phase via an inter- molecular as well as an intra-hydrogen bond. This means that cellulose will not melt before extreme exposure to thermal degradation (Fengel and Wegner et al. 1989). Cellulose monomers are also structured in parallel positions to each other in the fibrils, the cellulose fibrils are surrounded by a matrix of lignin and hemicellulose as shown on **Figure 2.2**. (Zimmerman and Pohler et. al. 2005).

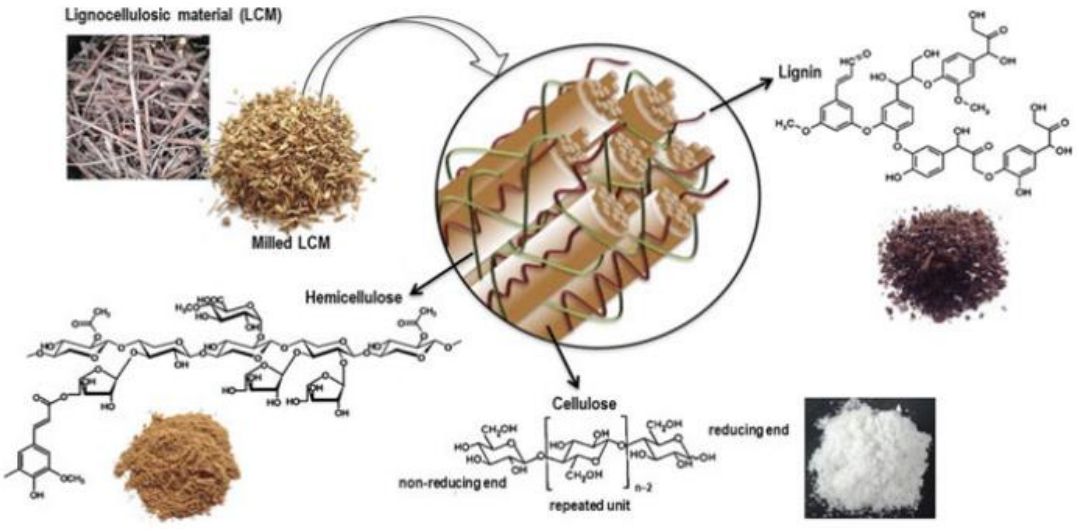

Figure 2.2: Graphical adaptation of fibrils showing hemicellulose, lignin and cellulose (Michelin et al. 2014).

The high fibre content in sugarcane bagasse seen **Figure 2.2** illustrates the matrix that cellulose exists in. The presence of hemicellulose and lignin in the complex is the reason behind the decreased accessibility to cellulose micro fibrils and is a hindrance to the isolation of cellulose. There are different morphologies of cellulose that are found in nature namely: cellulose I, II, III, IV and V (Wang et al. 2017). Cellulose I and II however are of high value to chemical industries due to their properties. Cellulose I and II are stable at high temperatures, consist of fibrils, possess high tensile strength, have luster and fabric smoothness to change when industrially applied. Cellulose I is the native cellulose and possess a chain that has a parallel arrangement, cellulose II however has an antiparallel chain (Ma et al. 2011).

The cellulose polymer is insoluble in most common solvents including water this is caused by the formation of multiple intra and inter-molecular hydrogen bonding (Valim et al. 2017). The majority of its biosynthesis happens in the walls of the plant cell. Four other sources which produce cellulose are animal, bacteria, chemical treatment and enzymes (Alberts et al. 2002). Recent developments have seen the use of cellulose fibres in the novel areas of materials science increase exponentially due to a major focus on the use of bio renewable resources, their permeative abundance and availability in various forms and most importantly their low cost (Gurunathan, et al. 2015).

2.3.1 Cellulose pre-treatment methods

Pre-treatment is essential for the separation of lignocellulosic material (LM) into its components. The extracted cellulose can then be converted to high value chemicals. This is due to the crystal lattice of cellulose, degree of polymerization (DP), level of moisture content and surface area that becomes available for chemical interactions and cellulose conversion into other compounds. The presence of lignin also hinders the process of hydrolysing agents on cellulose due to the matrix in which cellulose naturally occurs. These and other factors are overcome through the chemical pre-treatment methods.

Pre-treatment is mainly for separating cellulose fibres from lignin, aids the breaking of lignocellulosic structures and improves accessibility to cellulose chains. Pre-treatments can be

expensive, but they are necessary in the efforts to convert biomass into fermentable sugars and other high value products (Binod et al. 2002).

According to Binod et al. (2012) to ensure successful pre-treatment, pre-treatment methods should avoid:

- reducing the particle size of the biomass,
- degradation of the hemicellulose fractions,
- formation of large amounts of degradation products,
- high energy demands
- high costs,
- difficult and cumbersome processes,
- non-recyclable solvents for economical purposes.

2.3.2 Types of pre-treatment methods

2.3.2.1 Steam explosion

Steam explosion is a commonly used method in the pre-treatment of lignocellulosic biomass and can be executed with/without the use of a catalyst (alkali or acid). The ground biomass is treated with a concentration of a high-pressure saturated steam system, at temperatures ranging from 160-260 °C and pressure ranging at 0.69-4.83 MPa, the pressure is then reduced quickly, this then causes the biomass to experience an explosive decompression. The method causes a disruption in the materials structural composition, the fractional degradation of hemicellulose and lignin as a result of high temperature, this then makes cellulose available and it is then subsequently hydrolysed (Öhgren et al. 2007). A steam explosion treatment from Sundrop Fuels (2016) is shown in **Figure 2.3** below.

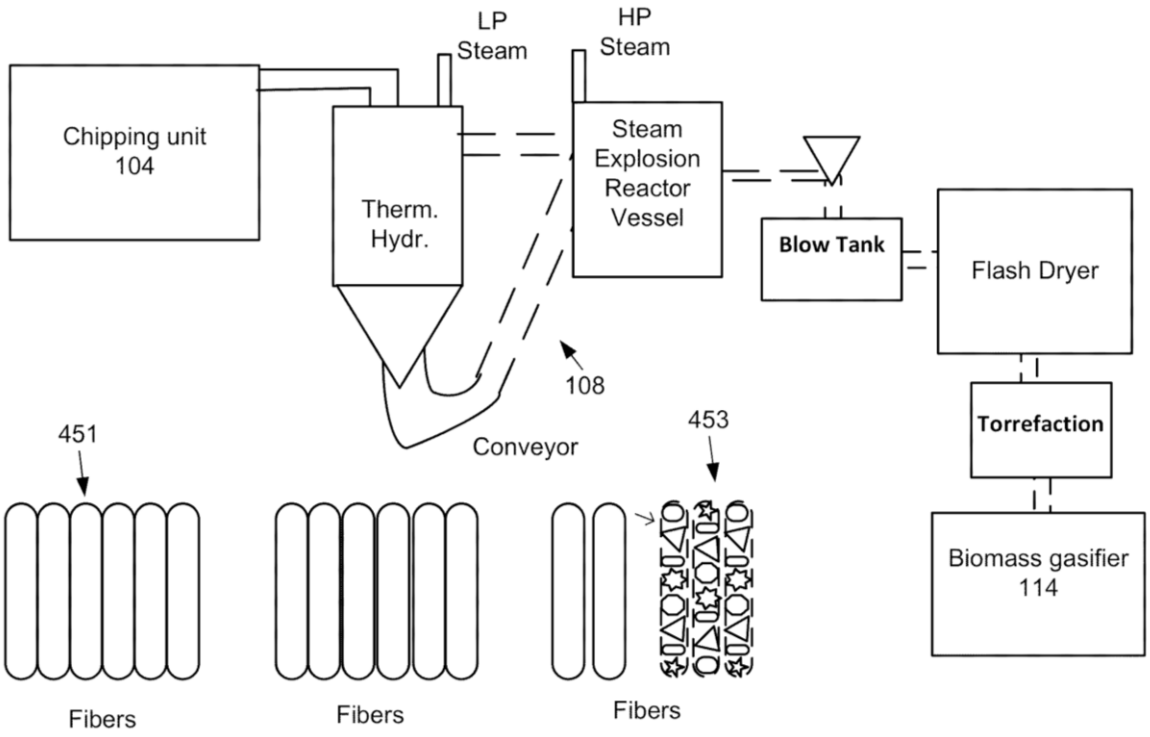

Figure 2.3: Graphical representation of the steam explosion pre-treatment technique (Sundrop Fuels. 2016).

2.3.3.2 Liquid hot water

Liquid hot water is solely a hydrothermal pre-treatment method. It is a method where pressure is applied to sustain water levels in the liquid state at high temperature ranges of 170 – 230 °C and a pressure of 5 MPa are frequently applied (Talebnia, Krakashev, Angelidaki et al. 2010). Liquid hot water when compared to water at ambient conditions have properties such as: high dielectric strength and greater ionic products which may be manipulated as a function of pressure and temperature to obtain the desired component. Liquid hot water can produce high yields of cellulolignin or lignin and minimum amounts of unwanted waste (Schact, Zetzl and Brunner et al. 2008).

2.3.3.3 Organosolv

The process of organosolv is derived from the treatment of samples with organic solvents also known as organosolvents and involves the use of an organic solvent and water. In this process the introduction of a catalyst, acid or alkali is not permitted. Organosolv related pre-treatments are basically used for the efficient removal of lignin from the lignocellulosic material through the fractional hydrolysis of lignin bonds, this results in a pulp that is rich in cellulose. The inclusion of a catalyst may enhance the selectivity of the organosolvent towards lignin. A large majority of the hemicellulose sugars may also be solubilized through this process (Mesa et al. 2011). This method is mainly advantageous to water-based processes. Separations are easily achieved by a distillation method with simultaneous re-use of the solvent (Novo et al. 2011).

2.3.3.4 Wet oxidation

This is mainly a hydrothermal type of treatment, it involves the use of water, air or even oxygen at moderately higher temperatures above 120 ˚C (McGinnis, Wilson and Mullen et al. 1983). During wet oxidation there are two main types of reactions that occur (Martin, Klinke, Thomsen et al 2007):

- A low hydrolytic reaction
- A high temperature oxidation reaction

In this method the cellulose is separated after the removal of hemicellulose and lignin (Jong and Gosselink et al. 2014)

2.3.3.5 Acid

The use of dilute acid hydrolysis is highly efficient and selective for the pre-treatment of sugarcane bagasse fibres. The pre-treatment specifically employing dilute sulphuric acid has been viewed as one of the more cost-effective methods if not the most cost-effective method. The combination of biomass and dilute acid mixture is generated at reasonable temperatures, the temperatures are controlled by using conventional heating or microwave sources (Galbe and Zacchi, 2002: Sanchez and Cardona, 2008: Tomas-Pejo et al. 2008). During this pre-treatment some polysaccharides are hydrolysed, many of those polysaccharides are hemicellulose fractions. The resultant free sugars are degraded to furfural, they also form 5-hydroxy-methyl-furfural (HMF) at higher temperatures, these products are inhibitors to the formation of microorganisms and their formation means the damage of fermentable sugars. Organic acids such as maleic and fumaric are suggested as alternatives to avoid HMF being formed (Koostra et al. 2009). The yield of cellulose is typically less than 20 % of the theoretical or expected value when pre-treatment methods are not implemented (Lynd et al 1996). However, pre-treatment increases the yield to significantly 90 % of the theoretical yield. The cellulose conversion of an acid pre-treated cane bagasse was 93.1 % using a 21 wt. % peracetic acid solution (Sanchez and Cardona et al. 2008).

2.3.3.6 Alkaline

The process of alkaline pre-treatment has recently become a common form of pre-treatment due to its ability to remove lignin from biomass. The subsequent removal of lignin increases the reactive nature of the residual polysaccharides which also aids the removal of the acetyl functional group and other uronic acids substitutions on hemicellulose (Chen, Ye and Sheen et al. 2012). The reaction mechanism of an alkaline hydrolysis is saponification of the intermolecular ester bonds that are cross linked with xylan hemicelluloses and other constituents such as lignin and other various hemicelluloses. Alkaline pre-treatment of lignocelluloses with dilute NaOH causes swelling of the material which results an increase in inner surface area, a decrease in degree of polymerization (DP) and crystallinity. It also leads to the degradation of chemical bonding and linkages between the lignin and carbohydrates and interference of the lignin constituency (Soccol and Vandenberghe et al. 2003).

2.3.3.7 Ionic liquid (IL)

Ionic liquids have also recently shown great promise as a method that could be used to pre-treat lignocellulosic materials (LMs). They are solvents which can be used for biomass dissolution with a high recovery of cellulose when an anti-solvent is added. Ionic liquids are organic salts that are liquid at room temperature and can be stable as liquids to temperatures up to 300 °C (Lee et al. 2009). 1-Ethyl-3-methylimidazolium acetate [Emim][OAc] is an example of one IL that can solubilize LMs and remove lignin, so that hemicellulose or cellulose can be recovered from the polysaccharides (Singh et al. 2009). The high solvating properties of ILs make them key in the dissolution of LMs and can be manipulated to extract a single constituent of LMs such as cellulose (Mora-Pale et al. 2011).

2.3.3.8 Mechanical

Tsapekos et al. (2018) showed that introduction of mechanical pre-treatment such as crushing and grinding of biomass can improve physical properties such as particle size of the starting material. Mechanical pre-treatment methods are conducive for industrial applications (Carrere et al. 2015). These methods heavily rely on the application of compression forces and this causes biomass deconstruction (Kratky and Jirout, 2011) as seen in **Figure 2.4**.

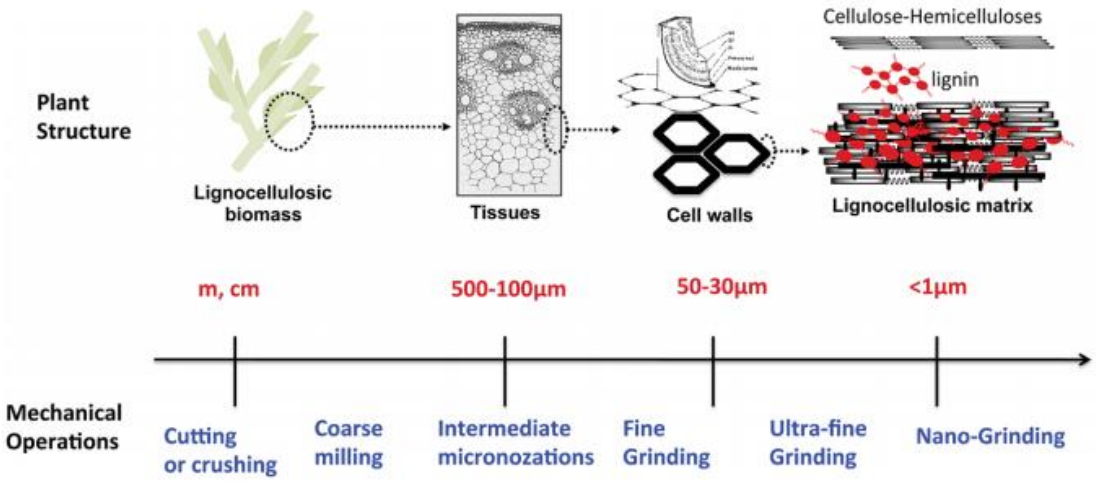

Figure 2.4: Mechanical pre-treatment of different materials and size reduction capacity (Barakat et al. 2014).

2.3.4 Applications of cellulose

Cellulose is a starting material that can be used for many applications. Cellulose I fibres have wide usage in industries such as clothing for fabrics, cosmetics and pharmaceuticals. Cellulose II is preferable in clothing when it comes to smart materials and biomedicine (Ma et al. 2011). Cellulose is used in the paper industry, where it is a structural material for paper and cardboard based products. The chemical modification of cellulose is a key step in synthesising cellulose derivatives which have further industrial applications.

2.4 Cellulose derivatives

Cellulose derivatives that arise from natural waste have shown diverse physio-chemical properties (Balser et al., 1986): such as solubility, adjustable viscosity and tensile strength (Klemm et al. 2005). Cellulose derivatives possess the ability to bond with a large range of substrates shown by the degree of polymerization (Balser et al. 1986). Cellulose derivatives are preferred in many industries such as food, cosmetic and textiles (Balser et al. 1986). Some cellulose derivatives through an etherification processes may be modified to be soluble in water (Olivas and Barbosa-Cánovas et al. 2005).

Cellulose derivatives gained a large significant industrial application as a smokeless gun powder (Kamel et al. 2008). These cellulose derivatives included methyl, hydroxyethyl (HE), hydroxyethyl methyl (HEM), hydroxypropyl (HP), hydroxypropyl methyl (HPM) and carboxymethyl (CM) cellulose. The synthesis of derivatives can be done by reacting a selective alkyl halide with cellulose that has been pre-treated with an alkaline solution. The cellulose used for synthesis of derivatives is conventionally obtained from biomass. Many substitution reactions can be undertaken by cellulose to form the ether derivatives (Kamel et al. 2008). The number of average R groups that is present in each glucan (polysaccharide from D-glucose) unit along the chain is the degree of substitution (DS). Physical properties such as solubility can be affected by DS and according to Rowe et al. (2013) the range of R groups present on glucan units is 0 – 3.

2.5 Carboxymethylcellulose (CMC)

Carboxymethyl cellulose (CMC) is one of the most significant derivative of cellulose, CMCs have many industrial uses in the production of materials we use daily. CMCs also have a long linear chain. CMC derivatives are water soluble and are anionic polysaccharides (Bono et al. 2009). The solubility of cellulose can be increased by the introduction of the carboxymethyl group (-CH_2COONa), this is done by replacement of the hydrogen of the OH unit that forms hydrogen bonds that make cellulose insoluble. CMC that has more than one substituent (-CH_2COONa) in a range of two glucose molecules as shown in **Figure 2.5** is soluble in water. The DS and the average degree of polymerization (DP) are alternative pathways that CMCs can be uniquely characterized (Batelaan and Ginkel et al. 1992). The DP is also known as the chain length which can be as high as 5000.

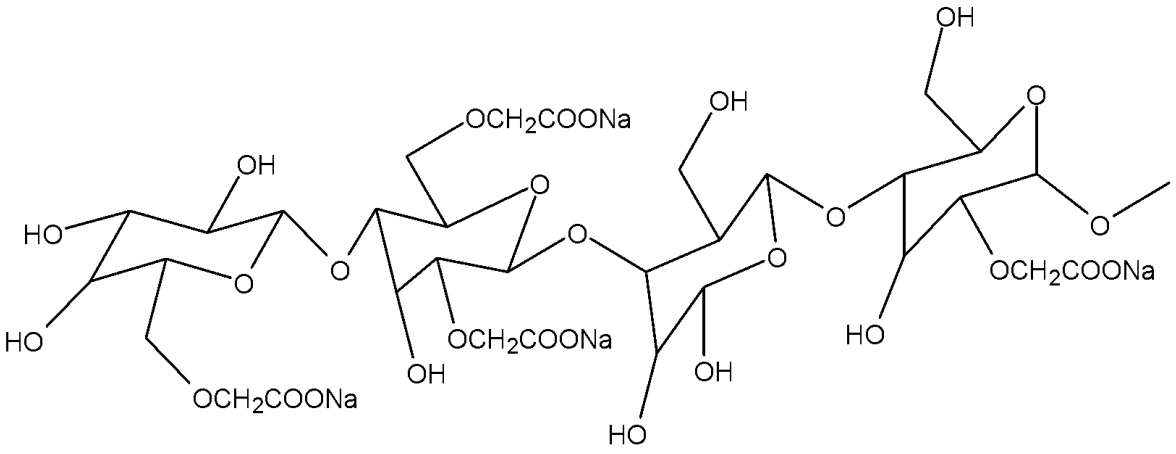

Figure 2.5: Molecular structure of carboxymethyl cellulose (Abouloula et al. 2018).

2.5.1 Properties of CMCs

2.5.1.1 Solubility

Carboxymethyl cellulose easily absorbs moisture, it is also very easy to dissolve in hot or cold water as a colloidal solution, and it may not be dissolved in many organic solvents such as methanol, ethanol, chloroform, acetone and all other similar solvents (SINOCMC. 2011a). The importance of the DS is that it also influences the water solubility of CMCs (Casaburi et al. 2018). Viscosity of the CMCs (25 mPa.s – 8000 mPa.s) also has a small impact on water solubility which is temperature and pH dependant (Sidley Chemical. 2013a; Sidley Chemical. 2013b). When the DS of CMCs is 0.4 or greater the solution shows alkaline solubility (SINOCMC. 2011a) The increase in DS improves the transparency of solution and the solubility increases (SINOCMC. 2011a). When CMC is being dissolved the first phase is expansion before it gradually dissolves. When preparing solutions, it is advisable for particles to be wet uniformly for a fast dissolution. This is used to avoid scattering of particles and this would lead to dissolution difficulties (SINOCMC. 2011b). There are grades of CMC that have been reported to need prior dissolution before application (Eliza et al. 2015).

2.5.1.2 Degree of substitution (DS) and morphology

The degree of solubility is known as a function of the DS (Lopez et al. 2015), this occurs when less substituted CMC which is more hydrophic shows a large fraction of aggregates. These aggregated crystalline domains were investigated using X-ray diffraction in aqueous solutions, the degree of crystallinity corresponds to a lower DS and little to no crystallinity was found at a DS of 1.06 and above. The regularity of substituting monomers instead of average DS was the main factor controlling rheological properties of CMC aqueous solutions (Lopez et al. 2015). Nanocomposites of CMC show the particles are spherical in shape, and at higher DS the particle size grows larger (Cui et al. 2011).

2.5.1.3 Factors that impact viscosity

The viscosity of CMC is dependent on the degree of polymerization (DP) of cellulose. Other factors that influence viscosity are the DP during alkalization, etherification and the homogeneity

of the reaction during synthesis (Sidley. 2015). The viscosity of CMC aqueous solutions rises linearly with an increase in concentration. Viscosity is also affected by pH, temperature and DS.

2.6 Synthesis of CMCs

Several techniques have been used to synthesise CMCs. These methods are:

- homogenous carboxymethylation (Heinze et al. 1999),
- fluidized bed technique (Durso et al. 1981),
- paddle reactor (Holst, Lask and Kostrezwa et al. 1978).

All techniques involve the use of an alkali-based substance that swells the cellulose, the swelling causes modifications in cellulose crystallinity and increases fibre accessibility. The steps of a carboxymethylation reaction as shown on **Figure 2.6** involve:

- Mercerization: Common method of synthesis is the slurry method, where: cellulose is mixed in a system that consists of NaOH, water and alcohol (ethanol or isopropanol) the reaction temperature is kept at a range of 20 – 30 ˚C and the alcohol should be in excess in the system this warrants a good mixing efficiency (Mann et al. 1998). The process where the liquid alcohol-water mixture which becomes a solvating agent and dissolution of the NaOH ensures its even distribution to the cellulose hydroxyl (-OH) groups forming the resultant alkali cellulose. The $NaOH_{(aq)}$ penetrates the crystalline structure of cellulose which solvates its hydroxyl (-OH) groups and this avails them for etherification (Savage, Young and Maasberg et al. 1954).
- Etherification: This process is also known as the Williamson Etherification (Tijsen et al. 2001) where the alkali cellulose that is synthesized is highly reactive to monochloroacetic acid (MCA), which is added to form a carboxymethyl cellulose ether (Kraasig et al. 1993).

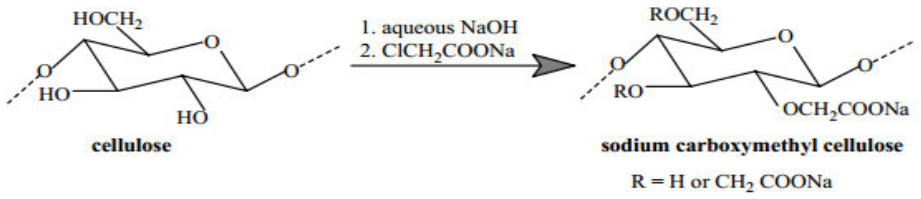

Figure 2.6: Carboxymethylation reaction of cellulose (Heinz and Pfeiffer et al. 1999).

2.7 Applications of CMC

CMCs have an extensive array of uses in many industries as the sodium salt (NaCMC), it is used extensively as a polyelectrolyte cellulose derivative. CMCs are anionic and water soluble which makes them preferable in applications such as food, pharmaceutical, personal care/ cosmetic and paper (Lopez et al. 2015). It may also be used in the production of other household products which include ice-cream, water paints and detergents (Toğrul and N. Arslan., 2003: Pushmalar et al., 2003). Industrially the use of CMCs has also been paper-based applications. CMC is non-toxic and has minimal cause of allergic reactions in the human body (Batdorf and Rossman et al. 1973).

2.7.1 Pharmaceutical industry

Out of all the cellulose derivative's only CMC is used in the preparation of further compounds. It is commonly accessible as a calcium or sodium crystallized salt in the form of polycarboxymethyl (CH_2COOX) where X = Ca or Na. CMC-Na is a capsule disintegrant, stabilizing, or suspending, or emulsifying (0.25-1%), or gel-forming (3-6%) and a viscosity increasing (0.1-1%) agent in compounded medicines. It has applications in oral (liquid, solid) and topical (liquid gel, emulsion) medicinal formulations, essentially for its viscosity-increasing properties. The more viscous CMC derived aqueous solutions are applied as a suspension powder for topical or oral purposes. In emulsions CMCs are an option to be used as stabilizers. Concentrations of CMCs with intermediate viscosity form gels which are used as a base product for cosmetics and other drug formulations (Rowe, Sheskey and Quinn et al. 2009).

2.7.2 Oil drilling

There is an oil drilling standard grade CMC made to be used as a separating fluid, drilling fluid as well as a strengthening fluid which is a fluid loss intermediate. CMCs also protect the shaft walls and hinder mud loss which increases recovery efficiency (Irochemical. 2015).

2.7.3 Ceramics

CMC in the ceramic industry is used as a gum and these gums maybe used in ceramics to harden the ceramic glazes and by so doing it cements the particles together and promotes safe handling of the ceramics (Hansen et al. 2015).

2.7.4 Insecticides

In mosquito coils CMCs ensure that it is mosquito repellent and it does so by evenly binding the ingredients. In the absence of elm powder CMC has a great moulding effect. It changes the appearance of the mosquito repelling incense making it brighter and cleaner. It also increases the chemical strength of the mosquito coil while physically enhancing its ability not to crack or break (Fortune Biotech. 2017)

2.7.5 Paper industry

CMCs have major functions in the paper manufacturing industry, however they are mainly used as strengthening agents. The CMC, the pulp and the filler agents have the same charge and properties it therefore increases the evenness of the fibre. The CMC also increases the bonding effects between fibres which improve on physical factors of the paper such as tensile and bursting strength of paper (Sidley. 2015).

2.7.7 Tobacco industry

Tobacco grade CMC is used in the industry for shaping, adherence and stabilizes the tobacco. The tobacco is also endowed by the CMC which is added (ZF Biochemical. 2016).

2.7.8 Mining industry

In the mining industry gangue slimes, which are normally clays and talc can be an issue due to bubble surface which crowd out copper mineral collection into bubbles. These slimes affect mineral recovery and overall mining conversion of the ore. The use of CMCs is to be a depressant of the gangues and ultimately conversion is improved (Danafloat. 2017).

2.8 Literature review of CMC production

The carboxymethylation of lignocellulosic materials has been extensively studied for the various properties that the products possess. The carboxymethylation process has generally been initiated with an aqueous alkali hydroxide, and the alkali cellulose is reacted with chloroacetic acid this process is referred to as the Williamson etherification synthesis and yields product CMC. The commercial production of CMC according to Balser et al. (1986) began in the early 1920's at the Farbenindustrie AG in Germany. Currently CMCs that have different applications and properties are tailor made and commercially available (Heinze and Koshella et al 2005).

There has been work previously reported where CMC obtained from different biomass resources is detailed. In this section we report some of these literature findings and highlight some of the results obtained. Mansouri et al. (2015) reported a novel synthesis of CMC from Tunisian vine stem (VS). The study involved delignification using two main pre-treatment methods to yield the products. The first pre-treatment of VS was with an aqueous soda solution (15 % w/w) at elevated pressure (3.6 bars) for a period of 2 hours. The fibres were then washed with water to neutrality before they were bleached with a sodium hypochlorite ($NaClO_2$) solution. After the treatment and at a pH of 12 fibres were washed with water to neutral and yielded approximately 40% of bleached cellulose product from vine stem (BF). The second step involved synthesising CMC directly from VS. The BF cellulose product would also be further carboxymethylated.

The method reported for the CMC synthesis from cellulosic material (VS and BF) is detailed by Aguir et al. (2010) and Khiari et al. (2011). Alkalization included the use of 30 mL of 40 % (w/v) NaOH followed by 30 mL of 1 butanol. Subsequently etherification was achieved by the addition of monochloroacetic acid (MCA) to the reaction mixture. The slurry was neutralized with acetic acid and purified with ethanol. CMC was successfully prepared from vine stems the yield and DS of the CMC product from BF was 75 % and 1.65, respectively. Direct CMC production from VS yielded 43 % CMC product with a 1.29 DS value. The study showed that cellulose production through delignification yields higher amounts of CMC than carboxymethylation of the biomass material directly. Mansouri et al. (2015) was able to compare these methods successfully. The study also focussed on the absorption (AC) retention capacities (RC) of the material adapted from Khiara et al. (2011) and Aliouche et al. (2000) and compared with commercial samples, which it found to be higher for prepared materials than commercially obtained CMC showing further advantages of the synthesis process.

In Brazil a study by dos Santos et al. (2015) investigated the regeneration of brewers spent grain (BSG), which is the main waste product of the brewery once beer is produced. An approximate mass of 15-20 kgs of BSG can be obtained per hectolitre of beer produced. The cellulose was extracted from BSG using alkaline treatment. BSG was treated with 2 % (w/w) aqueous NaOH for 2 h at 90 °C, thereafter the bleaching process employed with dilute (2 wt. %) $NaClO_2$. Bleached fibres were then neutralised with water and dried at 50 °C for 12 h in a circulating oven. The yield of cellulose product was calculated on a dry weight basis, where an initial 100 g of BSG yielded 15.37 g of dry pulp. The carboxymethylation steps were done with 0.5 g sample of bleached cellulose. Alkalization was done with isopropanol and 40 % (w/v) NaOH under magnetic stirring for 15 min at room temperature. The etherification reaction was carried out in a microwave reactor and MCA was dissolved in 2 mL isopropanol. The microwave irradiation was 200 W at a temperature range of (70-90 °C), stirred at an optimized time range (2.5 – 7.5 min). When microwave assisted irradiation was completed, the slurry was neutralized with glacial acetic acid and then filtered. The resultant CMC was washed with 70 % ethanol and dried in an oven.

Reaction conditions for CMC production were optimised, and all optimizations were done with respect to DS. A relationship between temperature, reaction time and MCA concentration was obtained from the reaction data.

The results from this optimisation showed that at increased reaction time and monochloroacetic acid wt. % loading there is an increase in the DS values. This was due to the carboxymethylation needing high concentrations of NaOH and MCA to increase carboxymethyl group substitution as reported by Barai et al. (1997). This observation was also supported by ^{13}C NMR which showed shorter cellulose chains due to higher substituted CMC groups. Thus, BSG has shown the potential to be a waste material that can be converted into CMC at optimal conditions of 5 g MCA /gram of cellulose, at a reaction time of 7.5 min and temperature of 70 °C having a DS of 1.46. This study displayed that the main factors that can be optimised on the etherification step CMC production are MCA concentration and reaction time as temperature did not significantly impact DS.

Heydarzadeh et al. (2009) also showed a new path towards CMC production from cotton fibres (CFs). The CFs were shredded, thereafter they were grinded and reacted in various NaOH concentrations (5-50 % w/v), excess NaOH was removed by filter press. Carboxymethylation was done by reacting the extracted cellulose with varied MCA (30-45 wt. %) concentrations. The mixture was reacted at 75 °C for a reaction time of 4 h with isopropanol and water as solvents. SEM images were discussed, and the images suggested that an optimum of 30 % NaOH (w/w) is ideal and external surface area showed that fibres we extensively methylated. The study showed that at varied concentrations of NaOH water and isopropanol have a linear relationship with DS. Isopropanol showed higher DS values than water, which was 0.7 and 0.55, respectively. The CMC sample obtained had a glossy appearance.

Sago palm is a readily available renewable natural polymer in Malaysia which is cheap, and biodegradable. Pushpamalar et al. (2006) showed a route towards CMC production from sago waste, the by-product of sago starch production. Sago palms produce sago starch which is an ingredient in food products (Doelle et al. 1998). The purification of sago waste pulp for CMC production involved drying of The material at room temperature for 3 h before grinding and sieving through a 0.5 mm^2 test sieve. It was further pre-dried at 60 °C for 1 h and was thereafter

suspended in hot distilled water with 1 mL of acetic acid, 1.5 g of $NaClO_2$ was then added in the flask and put in water bath for 3 h at 70 °C. The final residue was neutralised with distilled water and dried in an oven at 60 °C. A 5 g sample was reacted with 100 ml of solvent. The study also looked at solvent optimization with reference to the DS. The best solvent was further used optimized at varying ratios with water. Reaction time and MCA added per synthesis was varied. Sago waste was reacted by dropwise addition of 10 mL of 30 % (w/v) NaOH and stirred for 1 h. Carboxymethylation was done by addition of MCA at 45 °C under constant stirring for 3 h. The filtered product was soaked in 300 mL of methanol overnight. The methanol was then neutralised with glacial acetic acid and the CMC was oven dried to constant mass. Initial optimization showed that isopropyl alcohol at a water: solvent ratio of 20:80 gave a DS of 0.558. Continued optimisation of the process yielded CMC from sago waste yielded the best results at a reaction period of 180 min, 6 g of MCA, 10 mL 25 % (w/v) NaOH with isopropyl alcohol at a water: isopropyl alcohol ratio of 20:80 yielded a product with a DS of 0.821. These optimizations are advantageous because they give ideal working conditions and focus area for CMC production.

The study by Golbaghi et al. (2017) reports a novel route to pre-treat sugarcane bagasse (SCB) using steam explosion (SE) and subsequent carboxymethylation of the product cellulose to produce CMC and high molecular mass hemicellulose as a side product. Initially 100 g of SCB was put into a reactor where an aqueous solution of NaOH was fed in the reactor at a temperature of 170 °C – 190 °C with 250 rpm, for 30 min. When the SE pressure dropped defibrillated SCB broke down the to its components. For the isolation of cellulose 50 g of the pulp product in a reactor, was treated with a solution of H_2O_2 with at a pH = 13.5 and a reaction temperature of 55 °C. Equal volumes of H_2O_2 were added hourly for period of 3 h. The product was filtered and mixed with 1 M NaOH solution at room temperature for 3 h, post treatment the mixture was filtered and washed with double distilled water and the cellulose product was dried in an oven at 70 °C for 24 h. Cellulose was characterized by T-222 om-02, T-212 om-02 and Tappi 9 M-54 methods (Golbaghi et al. 2017). The presence of hemicellulose was detected by difference neutral detergent fibre (NDF) and acid detergent fibre (ADF). The difference between holocellulose and hemicellulose was used to calculate percentage cellulose content and the results reported 93.2 % cellulose content at 105 °C for 3 h.

For CMC production 1 g of cellulose was reacted with 1/20 (w/v) iso-propanol, followed by a slow dropwise addition of 4 mL (10 – 40 % w/v) NaOH (30 min) under stirring and the reaction time was 3 h at 25 °C. For carboxymethylation a mixture of MCA (0.5 g - 1.5 g) was dissolved in 20 mL of isopropanol and added dropwise in the mixture (15 min) reaction temperature and time were optimised at a temperature range (30 - 70 °C) and reaction time (1 – 6 h). The final product was filtered and soaked in methanol, neutralised with acetic acid, filtered and washed four times in absolute methanol to dissolve undesired products and finally dried in an oven at 60 °C for 12 h. The experimental results show that the dependency of DS on NaOH/MCA concentration. The DS of CMC increased and reached a maximum, then decreased at higher NaOH concentrations. At high MCA concentrations the DS increases and then reaches a plateau. Increase in reaction time and temperature increase the DS this is attributed to the longer reaction time allowing for more substitution reactions. Temperature is another contributing factor attributed to increased substitution reaction rates. The maximum DS that was obtained experimentally was 1.085 at a NaOH concentration of 28.4 g/dL, 1.14 g MCA, temperature of 57.85 °C and a time of 4.01 h. At the prementioned conditions a CMC yield of 181.302 % (m/m) was reported (Golbaghi et al. 2017). The results obtained from optimization had a good agreement to model prediction that was calculated showing that modelling can also positively impact this research area.

There have been many other sources of CMC from different biomass sources. Yaşar et al. (2007) showed a successful way to investigate the effect of viscosity on treatments for CMC from orange peels. Sugarcane straw (SCS) was used by Candido et al. (2016) for cellulose extraction by acid pre-treatment a 60 % product yield was observed, this produced a product with 2.72 DS. *Lantana camara* which is a type of weed plant was used by Varshney et al. (2006) MCA concentration and reaction time were optimized and the resultant effect on viscosity and DS was observed. At optimum conditions the CMC solution had a viscosity of 7500 cps (2 % solution) having a DS of 1.22 was reported. Toğrul et al. (2002) investigated the solubility and rheological properties of CMCs from sugar beet pulp. The DS of 0.67 was obtained for the optimized reaction. The study also highlighted that viscosity had a more visible effect on DS compared to temperature. The data could be further used in equipment design for handling CMCs in the parameters that were covered in the study.

CMC from bacterial cellulose was investigated by Casaburi et al. (2018), the study cultivated cellulose from glycerol and the product cellulose was successfully synthesised. The effect of optimization was shown using analytical techniques and a maximum DS of 1.44 was reported. Saputra et al. (2014) used water hyacinth which is an aquatic weed commonly found in Southern America and subtropical regions globally. The study focused on the variation of NaOH concentration for percentage yield calculations, and a maximum yield of 179 % was reported where solvent ratio optimisation was a key influence to product yield. Zhang et al. (2011) successfully used cotton stalk for cellulose extraction and produced CMC by microwave heating at 195.5 W microwave power for 1.97 min, this yielded a product with a DS of 0.765 and viscosity of 498 cps (2 % solution). *Posidonia oceanica* plants which accumulate every summer on the coasts of Tunisia were obtained by Aguir and Mhenni et al. (2005) for CMC production, the results shown for the bleached cellulose was a DS of 0.53 which improved to 2.75 through a three-step synthesis for etherification that was developed. *Ulva faciata* a green seaweed (Lakshmi, Trivedi and Reddy et al. 2017) showed the ability to produce CMC, at a DS below 0.4 the CMC was insoluble however at higher DS (0.51) the CMC was water soluble with a solution viscosity of 227 cps (2 % solution). Cavendish banana pseudo stem yielded a CMC product that had a DS of 0.75, a viscosity of 4033 cps (2 % solution) and 7.37 % crystallinity (Adinugraha and Marseno et al. 2005). Singh and Singh et al. (2013) proposed a viable route to produce CMC from corn cobic waste while Mondal et al. (2015) proposed a way to produce high purity food grade CMC from corn husks. Bamboo shavings (Chen and Lou et al. 2014), grapefruit peel (Karatas and Arslan et al. 2015) and wastepaper from everyday office use has been reported by Joshi et al. (2015) showing that there is constant ways to develop this particular research aspect.

In this work the extraction of cellulose from sugarcane bagasse was undertaken to produce CMC and this process involved the conversion of cellulose in aqueous sodium hydroxide and an organic solvent (typically ethanol or isopropanol) with monochloroacetic acetic acid (Heinze and Pfeiffer et al. 1999). Previous work focused on the physical and mechanical properties of the materials synthesised from biomass (Adinugaraha, 2005; Koh, 2013). This work however, focuses on the physio-chemical properties of cellulose and CMC using analytical techniques such as surface

morphology, particle size and crystallinity changes. Analytical techniques such as Attenuated Total Reflectance Fourier Transform Infra-Red (ATR-FTIR) Spectroscopy, Powder X-Ray Diffraction (PXRD), Scanning Electron Microscopy (SEM) and Transmission Electron Microscopy (TEM) were used. The characterization techniques used were to compare the experimentally obtained products to that of commercial analytical grade samples of cellulose and CMC. The results were also compared to those observed in the literature which were prepared using other bio-materials and pre-treatment methods. The chemical decomposition of the materials were also investigated by means of thermal studies, using Thermogravimetric Analysis (TGA) and Differential Scanning Calorimetry (DSC).

CHAPTER THREE

MATERIALS AND EXPERIMENTAL

3.1 Materials

The process used for the isolation of cellulose from hemicellulose and lignin will be described in this chapter. The dried mill-run sugarcane bagasse sourced from the Sugar Milling Research Institute in Durban was used as received. The first step in the process of CMC production was the removal of lignin and hemicellulose from the SCB fibres. The cellulose obtained was characterized and converted into CMC.

Most reagents used in this study such as Sodium hydroxide pellets, Nitric acid (37 %), Ethanol (99.99 %), Iso-propanol (99.99 %), Methanol (99.99 %), Monochloroacetic acid (MCA), Glacial acetic acid (99.99 %) and Phenolphthalein were of analytical grade unless otherwise specified and were all sourced from a local supplier (Capital Labs).

3.2 Experimental procedure

3.2.1 Cellulose extraction from sugarcane bagasse (SCB)

A process by Koh et al. (2013) described the extraction of cellulose from sugarcane bagasse for CMC production. This process however had short comings as in some cases it did not specify details such as ideal working conditions and concentrations of solutions that would produce the most effective results. Thus, a modification of the method was used in this work.

The sugarcane bagasse fibres were washed with 500 ml of distilled water. It was subsequently sun-dried for 24 hours. A 25.0297 g mass of sugarcane bagasse sample was weighed on an analytical balance (Ohaus) and transferred to a 5 L round bottom flask which was placed in a heating mantle (Electrothermal, Sweden). A 750 ml volume of 0.5 M NaOH (prepared by weighing 20 g of NaOH pellets in a 1 L volumetric flask) was transferred using a measuring cylinder into the round bottom flask and the resultant solution was heated at 70 ˚C for 15 min. After the initial heating the temperature was increased to 95 ˚C for 105 min. A dark slurry was then obtained. The slurry was filtered in portions until all the liquid from the solution was removed. The remaining solid product (cellulose) was washed with 1 L of distilled water.

Post-washing the resultant cellulose product was dried by means of vacuum filtration. The dried cellulose was refluxed for 60 min at 70 ^{o}C with two (approx. 200 mL) consecutive portions of a mixture containing 20 % (v/v) ethanol in nitric acid (80 mL of acid in 20 mL of ethanol: 80 % nitric acid). The 80 % (v/v) nitric acid solution (concentrated nitric acid in ethanol) yielded a residue that could not be quantified for further analysis. The experimental procedure was modified where less concentrated nitric acid solutions was used. A 8 M nitric acid solution was prepared by mixing 60 % of concentrated nitric acid with 40 % of water in a 500 mL volumetric flask. A 4 M nitric acid solution which was prepared by mixing 30 % concentrated nitric acid with 70 % of distilled water in a 500 mL volumetric flask. The mixture of cellulose and 20 % (v/v) nitric acid (8 M) in ethanol was then filtered and washed with 1L cold distilled water to a neutral pH of approximately 7, which was determined using a pH meter (Metrohm 781, Switzerland), to produce cellulose sample 1. The procedure was repeated for the 4 M nitric acid solution and produced cellulose sample 2.

It was important to neutralize the cellulose by decreasing the pH and washing off all the residual impurities. Thereafter the cellulose was dried overnight in a hot air oven at 30 ˚C. The dry cellulose was weighed, and the mass recorded to calculate the yield (m/m %). This process was done in duplicate measure for all cellulose samples extracted.

3.2.2 Percentage yield of cellulose

The mass of cellulose extracted from the sugarcane bagasse was determined on a dry weight basis. The yield of cellulose (%) was calculated using **Equation 3.1**.

$$\text{Yield of cellulose (m/m\%)} = \frac{mass\ of\ cellulose\ obtained\ (g)}{mass\ of\ bagasse\ used\ (g)} \text{ x } 100 \qquad (3.1)$$

3.2.3 Synthesis of carboxymethyl cellulose (CMC) from cellulose extracted from sugarcane bagasse (SCB)

The synthesis of CMC from the extracted cellulose was done in duplicate with an average mass of 1.0798 g cellulose sample 2, which was identified to give high yield at low acid strength and similar chemical composition to pure cellulose. Each sample was immersed in 30 mL of concentrated isopropanol the two reactants were mixed by means of continuous stirring using a magnetic stirrer bar on a hotplate in a 100 mL beaker. After stirring for a minimum time of 15 minutes, 15 ml of 20 %, or 25 % or 30 % (m/v) NaOH was added to different samples of cellulose sample 2. The 20 % NaOH solution was prepared by weighing 20 g of NaOH pellets on an analytical balance and transferring it into a 100 ml volumetric flask and bringing it up to the mark with deionised water. This procedure was done for the 25 % and 30 % NaOH solutions. The 20 % NaOH solution was cautiously added dropwise into the mixture, while stirring and further stirred for another 60 min. at room temperature. The carboxymethylation reaction was initiated upon addition of 1.2 g of chloroacetic acid under stirring (90 min). Thereafter the mixture was covered with aluminium foil and the beaker was placed into the hot air oven (60 ˚C) for 3.5 hours (Koh et al. 2013).

The slurry was subsequently soaked in 100 mL of methanol for 24 hours to further facilitate the carboxymethylation process. The slurry was then neutralized with the addition of an acetic acid

solution (20 % of acetic acid diluted with 80 % water) in small portions (10 – 15 mL) during filtration using a sintered glass crucible. The final product was washed three times by soaking in 10 mL of ethanol (10 min.) to remove undesirable by-products such as sodium glycolate and sodium chloride. The CMC product was washed again with 100 mL of absolute methanol. The final CMC product was filtered and dried at 60 ˚C to constant mass and kept in a desiccator. The mass of CMC was obtained by using an analytical balance (Ohaus). This procedure was done in duplicate for the 20 % (m/m). This procedure was also repeated in duplicate for the 25 % and 30 % NaOH solutions.

The yield of CMC was calculated from **Equation 3.2**. The yield of CMC synthesised was measured on a dry weight basis.

$$\text{Yield of CMC (m/m \%)} = \frac{Mass\ of\ dried\ CMC\ (g)}{Dry\ mass\ of\ cellulose\ (g)} \text{ x } 100 \qquad (3.2)$$

3.3 Degree of substitution (DS)

3.3.1 Titrimetric determination of degree of substitution (DS)

Triplicate 0.1 g samples of the dried CMC were weighed and ashed in a furnace (Ultrafurnace, South Africa) at 700 ˚C for a duration of 15-20 minutes. The ash samples were subsequently dissolved in 9 mL of hot de-ionised water and titrated with a 0.0500 M H_2S0_4 solution until the samples reached a pH of 4.4. The pH was tested using a pH meter (Metrohm 781, Switzerland) as described by Ambjörnsson (2013) and Hong et al. (1978). The potentiometric titrations were done in triplicate and the DS was calculated using **Equation 3.3** (Ambjörnsson. 2013; Hong. 1978).

$$DS = \frac{0.162\left(\frac{0.1\ b}{G}\right)}{1-0.080\left(\frac{.0.01\ b}{G}\right)} \quad (3.3)$$

Where:

b = mL of titration volume and

G = grams (g) of dried CMC used

0.612 = fraction of the molecular weight of the anhydroglucose unit

0.80 = fraction of the net increment in the anhydroglucose unit for every substituted carboxymethyl group

The application of CMC is characterized by a few factors and one being the number of substituted hydroxyl groups per anhydroglucose unit which has been described above as the DS (Torgul and Arslan et al. 2003). Potentiometric titration (Pushpamalar et al. 2006) is used to determine DS.

3.4 Characterization techniques

3.4.1 Attenuated total reflectance (ATR) - Fourier transform infrared spectroscopy (FTIR)

The attenuated total reflectance (ATR) – Fourier transform infrared spectroscopy (FTIR) (ATR-FTIR) technique was used for cellulose and CMC characterization. The sample of interest was radiated with a beam of light at different frequencies and the radiation was absorbed by the sample while some of it is passed through. The resulting spectrum was a representation of the absorption and transmission of light passing through at various wavelengths (Thermo Scientific. 2013). The spectrum is the raw data generated from analysis; this is processed by an algorithm called the Fourier transform. The spectra provides chemical functional group specificity, and this is arranged in a format that allows multiple bands that represent chemical functional groups to be tracked simultaneously from a single measurement (Ewing, Clarke and Kazarian et al. 2014). No two compounds may produce similar spectrums unless they themselves are similar or possess similar chemical bonds (Thermo Scientific. 2013). **Figure 3.1** is a typical FTIR spectrometer layout (Thermo Scientific. 2013)

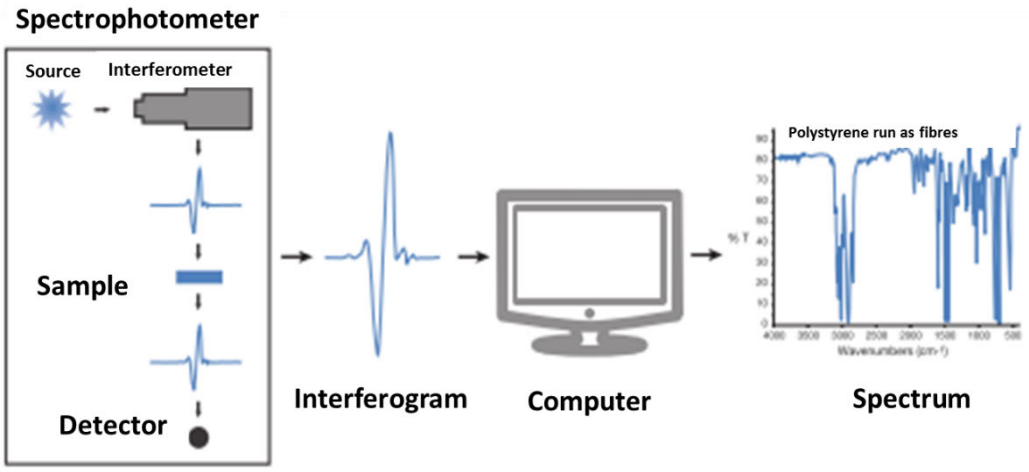

Figure 3.1: FTIR Spectrometer layout (Thermo Scientific. 2013)

In this work a Perkin Elmer (United States) 100 FTIR spectrophotometer equipped with an ATR unit was used for analysis. Cellulose and CMC samples were analyzed to observe functional group variations on the samples due to the chemical treatment processes that were done. The functional group changes were investigated. The ATR -FTIR spectra of the samples were recorded in the transmittance mode in the range of 4000 cm^{-1} - 500 cm^{-1}.

3.4.2 Powder X-ray diffraction (PXRD)

Samples for powder X-ray diffraction (PXRD) characterization are usually fine powder as the instrument measures the crystallinity of materials. This is achieved by measurement of the extent at which X-rays are different from planes of atoms within the sample. The instrument can be configured to use reflective, transmissive, divergent or, parallel beam optics. The Bragg equation (He and Preckwinkel et al. 2000) is closely related to the use of the PXRD as it is the key to calculating the 2-theta degree (Θ), which is plotted on the diffractogram. Braggs Law is defined by **Equation 3.4**.

$$n\lambda = 2d\sin\Theta \tag{3.4}$$

Where:

n = is an integer

λ = is the wavelength of the x-rays

d = space in between planes in atomic lattice of samples

Θ = the angle at which the sample is diffracted in degrees (He and Preckwinkel et al. 2000).

Shown below on **Figure 3.2** is a 2D XRD schematic diagram for powder samples.

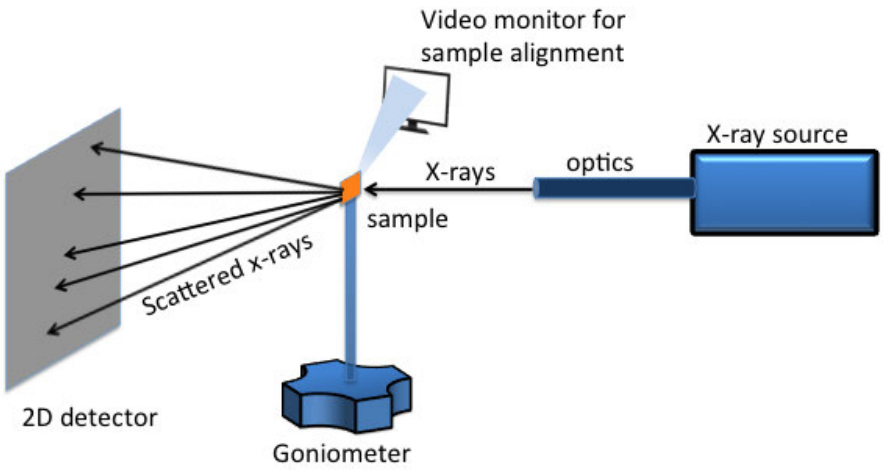

Figure 3.2: X-ray Diffractometer (He and Preckwinkel et al. 2000).

A PXRD (X'Pert Philips, United States) equipped with a Cu Kα radiation (0.1540 nm) polychromator beam in the 2θ scan range of 20 – 80 °C was used to elucidate diffractograms for the cellulose and CMC samples. A step time and step size of 87.63 s and 0.0170 (2θ) were used at 40 kV and 40 mA instrument power settings. The XRD patterns were obtained over the range 2θ = 10–30 ˚. The Scherrer equation (Monshi et al. 2012) on **Equation 3.5** was used to calculate the crystal size (nm) of cellulose and CMC samples in respect of the (200) plane.

$$L = K \lambda \beta_{1/2..} \cos\theta \qquad (3.5)$$

Where *K* is the correction factor and usually taken to be 0.91, λ is the radiation wavelength, ϑ is the diffraction angle, and $\beta_{1/2}$ is the corrected angular width (in radians) at half maximum intensity.

3.4.3 Thermogravimetric analysis (TGA)

Thermogravimetric analysis (TGA) is used to measure the change in sample weight with respect to the temperature. The instrument temperature is increased by a fixed amount (heating rate) to a set maximum. In this work a SDTQ- 500 (United States) thermogravimetric analyzer recorded the mass loss of cellulose and CMC samples over (25 – 600 ^{o}C) temperature range. The analysis was carried out at a heating rate of 10 °C/min. The instrument was purged with nitrogen (N_2) gas during the analysis at a flow rate of 100 ml/min. Figure 3.3 below shows the basic outline of a TGA.

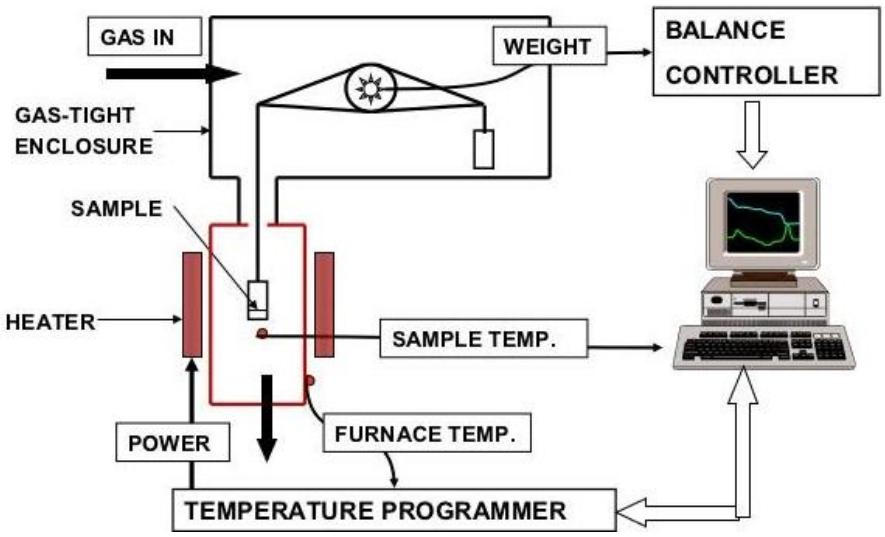

Figure 3.3: Thermogravimetric Analyser Outline (Price et al. 2012).

The thermobalance, a vertical rotating pivot represented by a balance controller on **Figure 3.3** is the electronic microbalance. The reaction takes place in a closed system to account for controlled pressure and general atmosphere surrounding the sample (Broido et al. 1969).

3.4.4 Differential scanning calorimetry (DSC)

The differential scanning calorimetry (DSC) instrument measures energy changes that occur when a sample is heated, cooled or is at a constant isothermal range. The energy changes allow for measurement of chemical-properties such as melting point, curing point, decomposition, and cooling point. DSC also allows for the measurement of subtle changes such as the glass-liquid transitions. One major advantage is the sample requires minimal to no pre-preparation.

The main unit of measurement in this instrument is the heat flow as a function temperature or time. The changes in heat that the instrument generates is highly dependent on the reference sample. It is important that a stable instrument response or baseline is obtained before sample changes are measured (Gabbot et al. 2008). **Figure 3.4** shows a schematic diagram that details the DSC instrument.

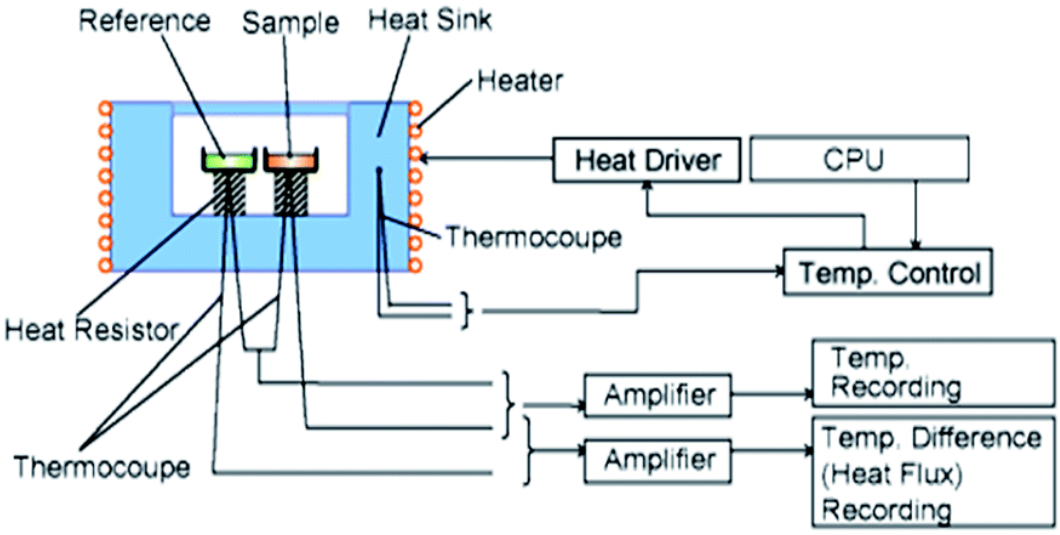

Figure 3.4: Differential Scanning Calorimeter (Bibi et al. 2015)

3.4.5 Scanning electron microscopy (SEM)

In scanning electron microscopy (SEM) information about the sample such as the surface morphology, crystallinity, and molecular dimensions are obtained. There are adaptations that have been made to SEMs that allow in-situ mechanical testing which show the behaviour of the material under various conditions. Typical SEMs need a high vacuum to operate.

In SEM a beam of electrons is constantly generated by a source which is a tungsten filament or a field emission gun, the electrons are accelerated by of extremely high voltages. The electrons then go through an array of apertures forming a beam which scans the top layer of the sample the sample emits electrons which are captured by the detector (WHD Microanalysis. 2017) shown more clearly on **Figure 3.5**.

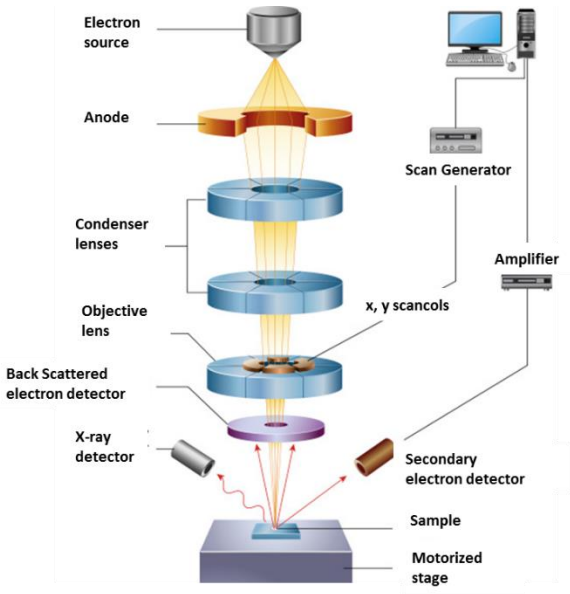

Figure 3.5: Scanning Electron Microscopy Layout (Inkson et al. 2016).

In this work the morphology of all cellulose and CMC samples were obtained using a JOEL-Jem (Japan) SEM equipped with an EMFC6 microscope, images were taken at different magnifications. The sample pre-preparation was done by spraying a fine layer of gold by an ion sputter coater with a low deposition rate.

3.4.6 Transmission electron microscopy (TEM)

The transmission electron microscope (TEM) may show images beyond the range that the naked eye can detect, its magnification may go up to 1 x 10^6. It achieves this by the production of electron diffraction patterns that are used to gain information on the crystalline material. Similar to SEM an electron gun produces electrons which now form a lens using the electron beam on the instrument. The TEMs imaging programme has three lenses that form a diffraction pattern of the sample on a light screen the configuration of the pattern on the screen together with the integrated camera detect the images that the instrument generates (Egerton et al. 2005). A schematic of a TEM apparatus is given in **Figure 3.6**.

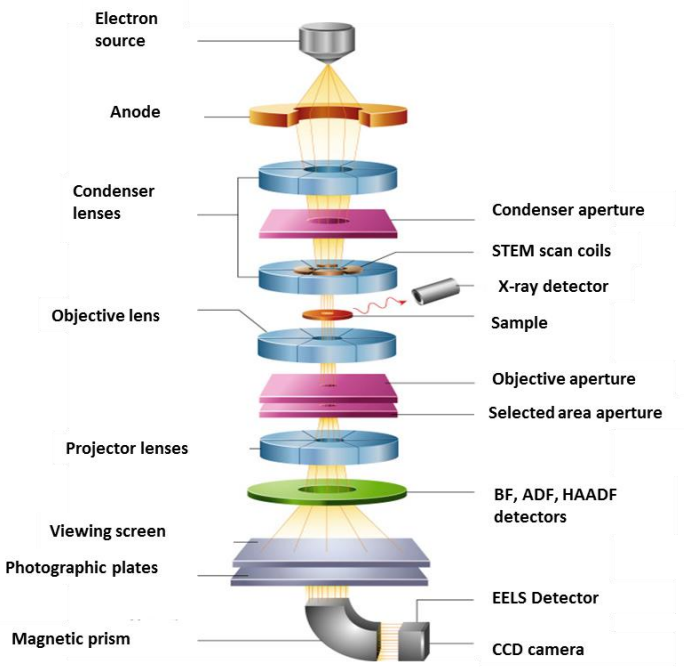

Figure 3.6: TEM Layout Adapted From (Inkson et al. 2016)

The TEM images were captured using a JEOL-Jem 2100 (Japan) with a Leica EMFC6 (LN2 attachment) microscope. Before images were taken dilute aqueous suspensions of all cellulose and CMC samples was sonicated and placed on a carbon copper grid where it could dry at room temperature. The surface morphology of cellulosic fibers and CMC was examined using field emission scanning electron microscopy.

CHAPTER FOUR

RESULTS AND DISCUSSION

This chapter outlines the results obtained on the production of carboxymethyl cellulose from cellulose. The latter was extracted from sugarcane bagasse biomass waste material.

Cellulose was extracted at various nitric acid concentrations. The CMCs were produced at different NaOH concentrations. Characterization of the products employed techniques such as Fourier Transform Infra-red (FTIR) spectroscopy, X-ray Diffraction (XRD), Thermal analysis (TGA), Electron Microscopy (TEM), among other analytical techniques.

4.1 Carboxymethyl cellulose production from biomass

4.1.1 Cellulose extraction

Figure 4.1a - **b** shows images of the commercial cellulose and extracted cellulose sample 1, respectively.

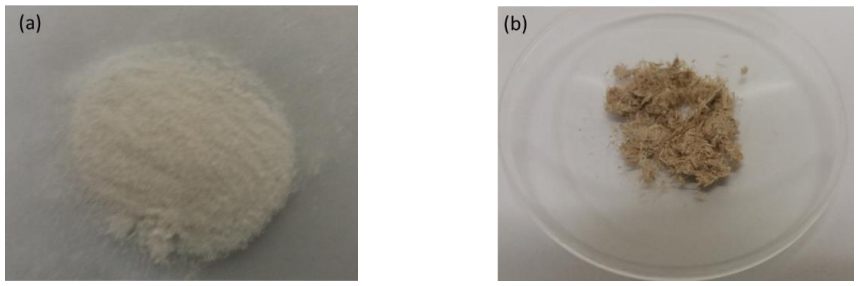

Figure 4.1: Photograph of pure cellulose (a) and (b) extracted cellulose.

The extracted cellulose sample was light brown due to residual lignin in the sample. This could also be due to the chemical pre-treatment method used. The bleaching done by most industrial processes differs from the laboratory scale pre-treatment done in this study. The chemical pre-treatments that yield a product which has similar physical appearance to commercial cellulose from a sugarcane bagasse sample is detailed by Mashego et al. (2016). Pushpamalar et al. (2006) produced CMC from sago waste and the sago pulp (cellulose) was bleached and yielded a sample that had a similar physical appearance to commercial cellulose as seen on **Figure 4.1**.

4.1.2 Effect of nitric acid concentration on cellulose yield

When the concentrated nitric acid (37 % v/v HNO_3) solution was used no cellulose was obtained. The strong acid completely solubilised the cellulose. Harsh acids lead to the degradation of sugarcane bagasse during pre-treatment and the formation of char (Skiba et al. 2017). Balat (2011) expanded on the several advantages and disadvantages of concentrated acid (sulphuric acid) pre-treatment and Liu et al. (2012) has attempted to used sulphuric acid and study its effects on saccharification on sugar recovery which was successful.

In this work, when 8 M and 4 M HNO_3 solution concentrations were used, and cellulose was successfully extracted from the sugarcane bagasse. The isolation of cellulose from sugarcane bagasse using the dilute 8 M and 4 M nitric acid solutions yielded 37 (m/m) % and 40 (m/m) % of cellulose sample 1 and cellulose sample 2, respectively. From **Equation 3.1** the yield of cellulose was calculated. A sample calculation is shown below for cellulose sample 1:

Yield of cellulose sample 1 (m/m%) $= \frac{Mass\ of\ cellulose\ obtained\ (g)}{Mass\ of\ bagasse\ used\ (g)}$ x 100

$= \frac{9.1678\ g}{25.0297\ g}$ x 100 = 36.63 %

The standard deviation for cellulose samples 1 and 2 were calculated using **Equation 3.1** (Garland and Tripathi et al. 1971).

$$\sigma = \sqrt{\frac{1}{N}\sum_{i=1}^{N}(x_i - \mu)^2}. \qquad (3.1)$$

Where:

σ = population standard deviation

μ = the population mean

x_i = each value of the population

N = the size of the population and Σ = The sum of the population

Table 4.1 shows the results obtained for cellulose yields for the duplicate samples of 8 M and 4 M nitric acid together with the standard deviations.

Table 4.1: Yield of extracted cellulose at 8 M and 4 M nitric acid.

Mass of sugarcane bagasse/ (g)	Mass obtained/ (g)	Cellulose Yield (m/m%)	Average Cellulose Yield (m/m%)	Std. dev.
Cellulose sample 1 (8 M HNO_3)				
25.0180	9.1678	36.60	36.63	0.285
25.0117	9.0120	36.03		
Cellulose sample 2 (4 M HNO_3)				
25.0033	9.8823	39.52	39.88	0.355
25.0066	10.0603	40.23		

At a higher nitric acid concentration, a decrease in cellulose yield from sugarcane bagasse was observed. Manaf et al. (2018) investigated the effect of varying dilute nitric acid concentration (0.5 – 7 % v/v) for the fractionation of biomass in the production of xylitol from lignocellulosic material (LM). Their study showed that the acid hydrolysis of LMs solubilizes hemicellulose and thus causes a degradation of ester bonds ultimately disintegrating the lignin-hemicellulose fractions (Sun et al. 2004). Similar to the trend that we have observed, Rodriguez-Chang et al. (2004) obtained a lower glucose yield of 2.87 g glucose/L when the concentration of HNO_3 was increased. Based on the study by Skiba et al. (2017) when dilute nitric acid (4 m/m%) was used to pre-treat oat hulls, cellulose pulp was obtained.

The yield of the cellulose obtained was calculated and found to be approximately 40 % for cellulose sample 2 where 4 M HNO_3 was used. The maximum yield of cellulose (40 %) obtained

correlated with the sugarcane bagasse compositional analysis done by Chambon et al. (2018) which stated that sugarcane bagasse fibres had 43 % of cellulose. Therefore, there was a 93 % extraction of the cellulose.

Only the cellulose sample 2 product was used for CMC production due to the slightly higher yields of the cellulose. From **Table 4.1** the cellulose yields showed an increase with a decrease in HNO_3 concentration for all samples similar to the work done by Abdul-Manaf et al. (2018).

4.1.3 CMC synthesis

Abdel-Halim et al. (2015) detailed how the carboxymethylation process is done. It is a two-step process that is detailed in Chapter 2 section 2.6. In this process water is used as a solvating agent to aid the even distribution of NaOH and direct it to the cellulose hydroxyl groups for the formation of alkali cellulose. The alkali cellulose is synthesised by NaOH penetration of the crystalline areas of cellulose and hydrogen bonds are broken which enables the hydroxyl groups for etherification. The monochloroacetate is then added to the alkali cellulose in its salt form to produce the sodium salt of the CMC ether, simultaneous etherification may lead to the side product formation of sodium glycolate and NaCl. The Williamson (Zhang et al. 2011) alkalization and etherification process of cellulose is shown in **Equation 4.2** and **4.3**, respectively (Zhang et al. 2011).

Alkalization:

$$[C_6H_7O_2(OH)_3]_n + nNaOH \longrightarrow [C_6H_7O_2(OH)_2ONa]_n + nH2O \quad (4.2)$$

Etherification:

$$[C_6H_7O_2(OH)_2ONa]_n + nClCH_2COONa \longrightarrow [C_6H_7O_2(OH)_2OCH_2COONa]_n \quad (4.3)$$

The CMC yields were calculated using **Equation 3.2** and are reported on **Table 4.2**. A sample calculation of CMC yield is given for cellulose sample 2 at 20 % NaOH (m/v):

$$\text{Yield of CMC (m/m\%)} = \frac{mass\ of\ dried\ CMC\ (g)}{mass\ of\ dry\ cellulose\ (g)} \times 100 = \frac{1.2205\ (g)}{1.0024\ (g)} \times 100 = 121.76\ \%$$

The CMC yield for the different NaOH concentrations is shown in **Table 4.2**.

Table 4.2. Percentage yield (m/m %) of CMC from cellulose sample 2 at varying NaOH concentrations.

Sample number	Dried cellulose (g)	Average cellulose (g)	NaOH Conc./ Mass of dried CMC (g)	Average CMC (g)	Yield (%)	Average Yield (%)	Std dev.
20 % NaOH (m/v)							
1	1.0022	1.0024	1.2200	1.2205	121.73	121.76	0.02
2	1.0026		1.2209		121.77		
25 % NaOH (m/v)							
1	1.0090	1.0098	1.2767	1.2870	126.53	126.59	0.06
2	1.0106		1.2793		126.65		
30 % NaOH							
1	1.0006	1.0008	1.4058	1.4099	140.50	140.87	0.36
2	1.0010		1.4140		141.23		

There is a linear relationship shown in **Figure 4.2** (where $R^2 = 0.9242$) between the concentration of NaOH and the yield of CMCs. Abdel-Halim et al. (2018) studies the carboxymethylation of the cellulose derivative hydroxypropylcellulose (HPC) to hyroxypropylcarboxymethylcellulose (HPCMC). The reported yields of HPCMC was 173 %, 190 % and 200 %, respectively at an increasing NaOH concentration. Joshi et al. (2015) optimised the carboxymethylation of wastepaper where an optimized concentration of 0.094 M NaOH and 0.108 M sodiummonochlorate (NaMCA) produced 150.8 (m/m%) CMC. The monochloroacetic acid and NaOH interactions promotes the etherification process and hence the CMC yields (Selke et al. 2004). The initial swelling of cellulose is observed in the alkalization process and this makes the pores of the cellulose fibre more susceptible for the substitution of the hydrogen in the hydroxyl group (-OH) with Na ions.

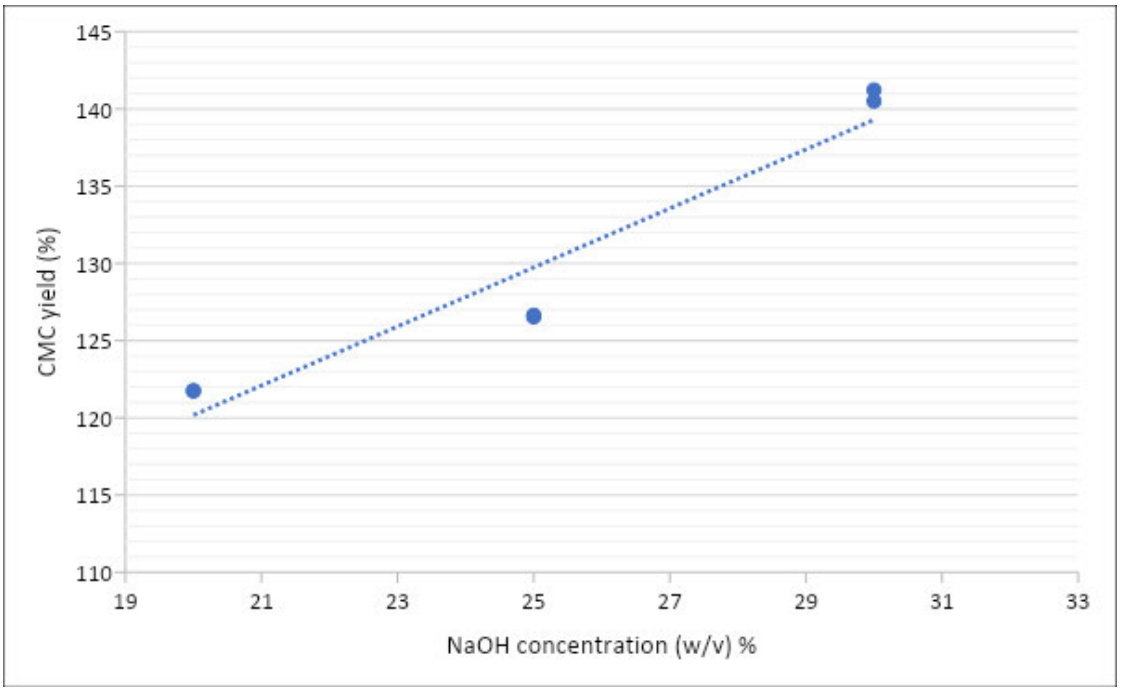

Figure 4.2: Graph of CMC yield vs NaOH concentration.

The etherification process allows for the replacement of Na ions with the carboxymethyl group (-CH_2COONa) as shown on **Equations 4.2** and **4.3**. The substituent groups coordination to the cellulose monomer results in a mass increase greater than 100 %. The high percentage loading of the alkaline solution however seems to be the main factor that causes increases in the yield. Koh et al. (2013) did a similar synthesis using sugarcane bagasse and further confirmed that an increase in yield of 113 %, 127 %, 145 % and 152 % for 10, 15, 20, 25 and 30 % (w/v) NaOH, respectively.

4.2 Characterization

4.2.1 Fourier transform infra-red (FTIR) spectroscopy

4.2.2.1 Cellulose

Figure 4.3 is the spectra obtained for commercial cellulose (a), cellulose sample 1 (b) and cellulose sample 2 (c).

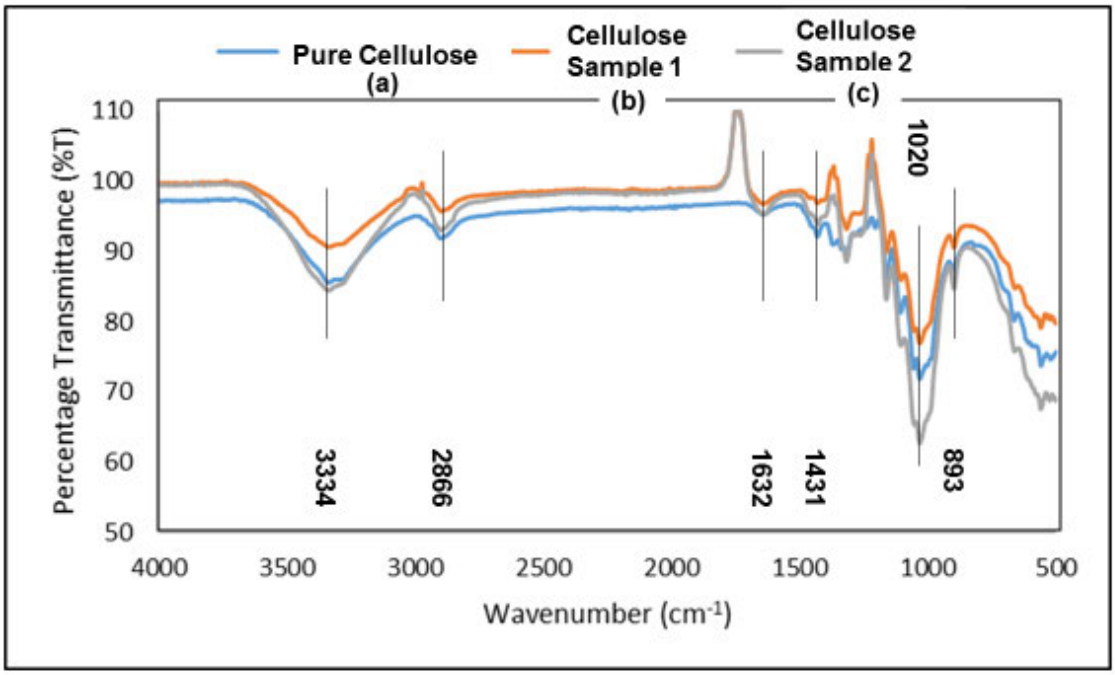

Figure 4.3: FTIR spectra of commercial and extracted cellulose.

The spectra in **Figure 4.3** are super imposed on each other to clearly show relative peak proximity to the pure cellulose sample. As illustrated in **Table 4.3**, peaks at the 3306 - 3334 cm^{-1} region show identical positions for all spectra, which indicates that the cellulose samples 1 and 2 are the same as the pure cellulose sample—a similar finding was observed by Mansouri et al. (2015).

Table 4.3. Peaks assigned for the spectrum shown on **Figure 4.3** for all cellulose samples.

Cellulose	Peak frequency (cm^{-1})	Peak attribution
Figure 4.2a		
Commercial	3334	OH, stretching vibration it is also a key indication that a bond formation has occurred.
	2866	C-H stretching vibrations.
	1420 – 1430	Symmetric CH_2 bending vibrations.
	1632 – 1642	absorbed H_2O band, -OH bending of water.
	1374	CH_2 group presence.
	1000 - 1200	C-O vibration band that corresponds to carbohydrate presence.
	898	C-O-C stretching at the glycosidic β (1-4) linkages, characteristic of cellulose.
Figure 4.2b		
Sample 1	3306	–OH, stretching vibration.
	2875	C-H stretching vibrations.
	1428	symmetric CH_2 bending vibrations.
	1631	absorbed H_2O band, -OH bending of water.
	1067	C-O vibration band.
	896	C-O-C stretching vibrations, glycosidic β (1-4) linkages characteristic of cellulose.
Figure 4.2c		
Sample 2	3331	–OH, stretching vibration.
	2887	C-H stretching vibrations.
	1428	symmetric CH_2 bending vibrations.
	1644	C-O vibration band.
	898	C-O-C stretching vibrations, glycosidic β (1-4) linkages characteristic of cellulose.

4.2.1.2 Carboxymethyl cellulose

The FTIR Spectra for CMCs produced from extracted cellulose (b-e) for commercial CMC (a) and 20 % (b), 25 %i (c), 25 %ii (d), and 30 % (e) NaOH are given in **Figure 4.3**.

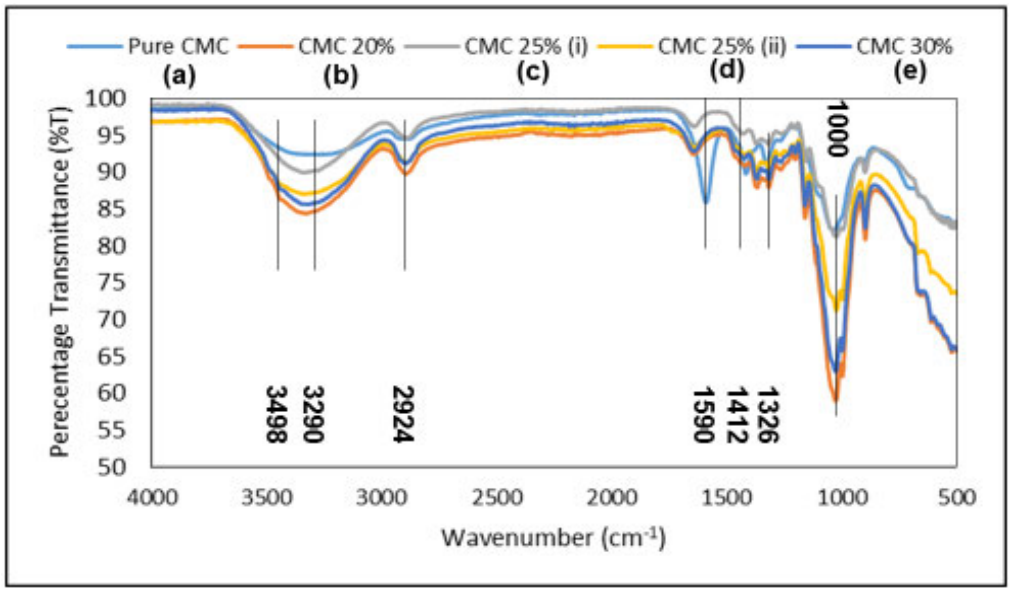

Figure 4.3: FTIR spectra of for commercial CMC (a) and 20 % (b), 25 %i (c), 25 %ii (d), and 30 % (e) NaOH CMC samples.

The spectrum for commercial CMC is seen on **Figure 4.3a**. Peaks identified in the spectra demonstrate the defining peaks corresponding with the carboxymethyl substituent in CMC. **Figure 4.3a** showed, for commercial CMC peaks at 1412 cm^{-1} and at 1590 cm^{-1}. The 20% NaOH CMC in **Figure 4.3b** showed similar peaks at 1416 and 1631 cm^{-1}, respectively. The 25% NaOH CMC from cellulose sample 1 in **Figure 4.3c** showed these peaks at 1439 and 1631 cm^{-1}, respectively. **Figure 4.3d**, 25 % NaOH CMC from cellulose sample 2 and **Figure 4.3e** for 30 % NaOH CMC showed a peaks at 1641 cm^{-1} and 1428 cm^{-1}. Peaks in the 1614 cm^{-1} region are important in FTIR characterization due to the peak being mainly attributed to carboxymethylation ($-COO^{-}Na^{+}$) as described by Joshi et al. (2015). This peak is accompanied by the broad band at 3290 cm^{-1} which is clearly seen on all the spectra in **Figure 4.3**. A peak in the 3400 cm^{-1} region is attributed to the presence of a hydroxyl group (-OH). The peaks at 2920 cm^{-1} are due to the C-H stretching

vibration (Mandal et al., 2018). All synthesized CMCs showed similar functional groups stretching and vibrations similar to that by Adinugraha et al. (2005).

4.2.2 X-ray diffraction (XRD)

4.2.2.1 Cellulose

The X-ray diffractograms in **Figure 4.5** show diffraction patterns of commercial cellulose and cellulose samples 1 and 2.

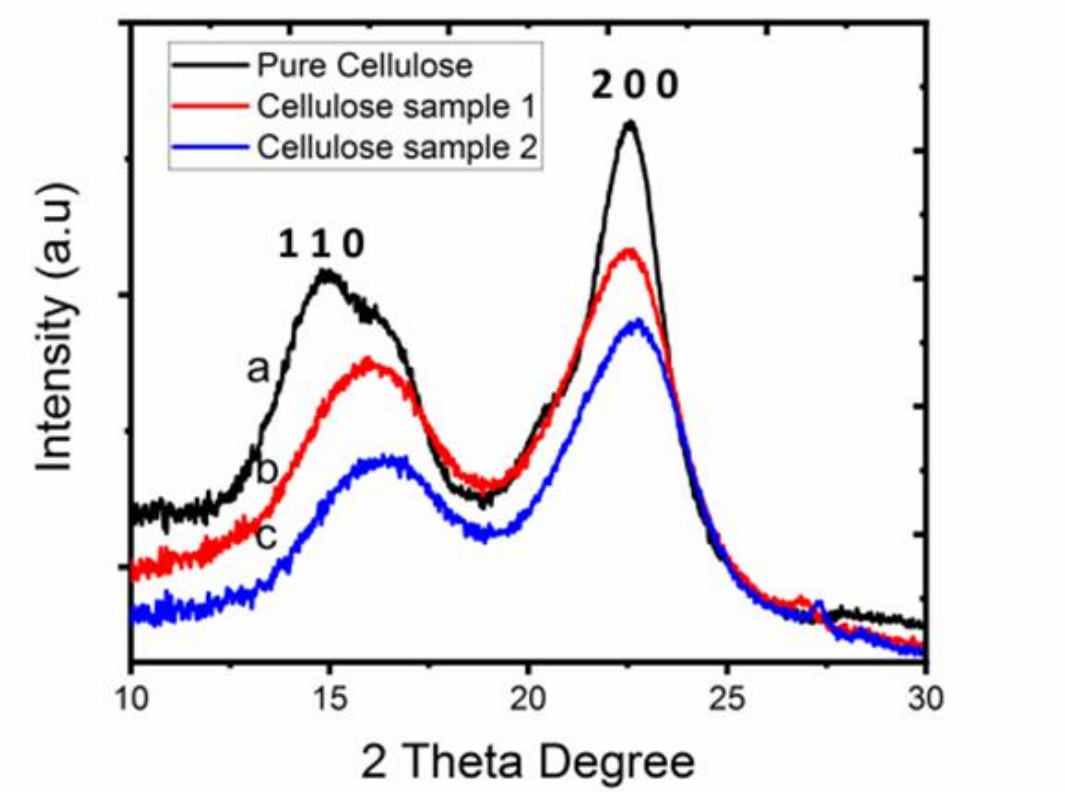

Figure 4.5: XRD of pure cellulose (a), cellulose sample 1 (b) and cellulose sample 2 (c).

The XRD patterns in **Figure 4.5a** - **c** for cellulose samples show diffraction peaks in the (1 1 0) and (2 0 0) planes corresponding to the respective *hkl* values for each sample. The three samples showed slightly broad peaks at 15˚ which are characteristic of crystalline cellulose crystal plane (1 1 0). The presence of cellulose can be attributed to the less intense peak at 2Θ = 15˚.

The diffractograms also shows a measurement at 2Θ = 23˚ (2 0 0 plane). Shankar and Rhim et al. (2016) have attributed the most intense peak on the 2 0 0 plane similar to those observed in **Figure 4.5** to the presence of cellulose I. **Figure 4.5a** shows fewer broad peaks for commercial cellulose compared extracted cellulose due to smaller granules found in crystalline analytical grade cellulose Mondal et al. (2015). Commercial cellulose also showed a more intense peak at 2Θ = 23˚ than cellulose samples 1 and 2. This may be indicative that the extracted cellulose was not as pure as the commercial cellulose. A similar finding was also observed by de Oliviera et al. (2011) when comparing crystals to fibres of similar materials.

These results confirmed the presence of cellulose which is highly crystalline. The broad peaks also correspond to the large crystallite structure of the cellulose (Lakshmi et al. 2017: Soykeakbew et al. 2009)

4.2.2.2 Carboxymethyl cellulose

Figure 4.6 shows the XRD of commercial CMC (a), 20 % NaOH CMC (b), 25 % NaOH CMC from cellulose sample 1 (c), 25 % NaOH CMC from cellulose sample 2 (d) and 30 % NaOH CMC (e).

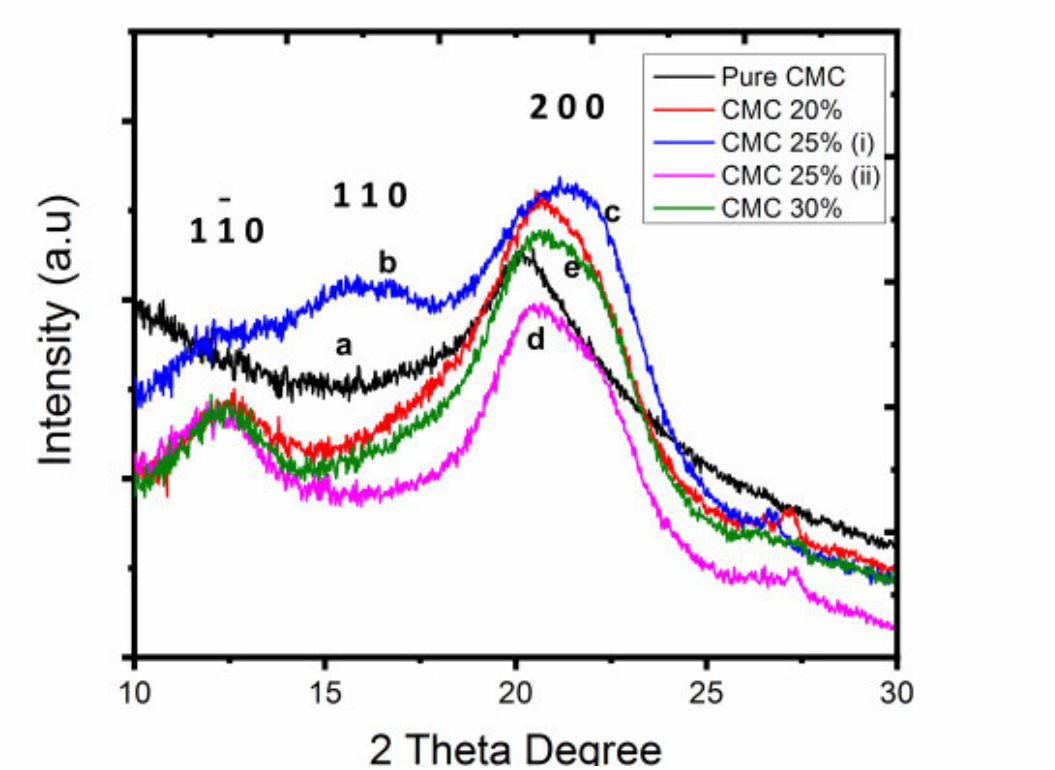

Figure 4.6: XRD patterns of commercial CMC (a), 20 % NaOH CMC (b), 25 % NaOH CMC from cellulose sample 1 (c), 25 % NaOH CMC from cellulose sample 2 (d) and 30 % NaOH CMC (e).

CMC XRD data tends to diffract differently when contrasted with cellulose. This is due to the etherification process and carboxymethyl bond formation due to substitution which affects the chain length (Abdel-Halim et al. 2015) and morphology. Commercial CMC showed no peak for the (1 1 0) crystal plane (**Figure 4.6a**) when compared to the synthesised as seen in **Figure 4.5**. The 25 % NaOH CMC samples showed a low intensity but sharp peak at 7.5˚ possibly indicating residual cellulose that wasn't converted to CMCs. The peak for commercial CMCs corresponds to the basal d spacing for crystalline materials with dimensions of 3.94 Å and 11.85 nm when calculated by Mandal et al. (2018) who interpreted an XRD of a CMC sample synthesised from nanocellulose (NC) for bio-composite CMC films in packaging and polymer industries. The peak

at the (2 0 0) crystal plane for commercial CMC was observed at 2Θ = 20.33˚. The peaks in **Figure 4a** – **e**, are comparable and indicate that CMCs have been synthesised (Almasi et al. 2010). The CMC XRD patterns on **Figure 4**.**5c** – **e** showed peaks at 2Θ = 20.86˚, 24.78˚ and 20.29˚ for 25 % NaOH from cellulose sample 1 (i), 25% NaOH CMC from cellulose sample 2 (ii) and 30% NaOH CMC, respectively. Due to the similarity of the diffraction patterns and pre-treatment methods all synthesised CMC samples exhibited similar peaks. Mandal (2018) and Mondal et al. (2015) produced CMC with characteristic peaks at 2Θ = 22.5 and 22˚ respectively which we have observed. However, Joshi et al. (2015) reported a single peak at 2Θ = 20.5˚ when CMC was synthesized from Brewers spent grain (BSG). CMC is less crystalline than cellulose due to the longer polymer chains in cellulose when compared to CMC. The decrease in crystallinity can also be attributed to the NaOH pre-treatment which causes hydrogen bond cleavage (Adinugraha et al. 2005)

4.2.3 Thermogravimetric analysis (TGA)

4.2.3.1 Cellulose

Figure 4.6 shows the thermograms of commercial cellulose (a), cellulose sample 1 (b), and cellulose sample 2 (c).

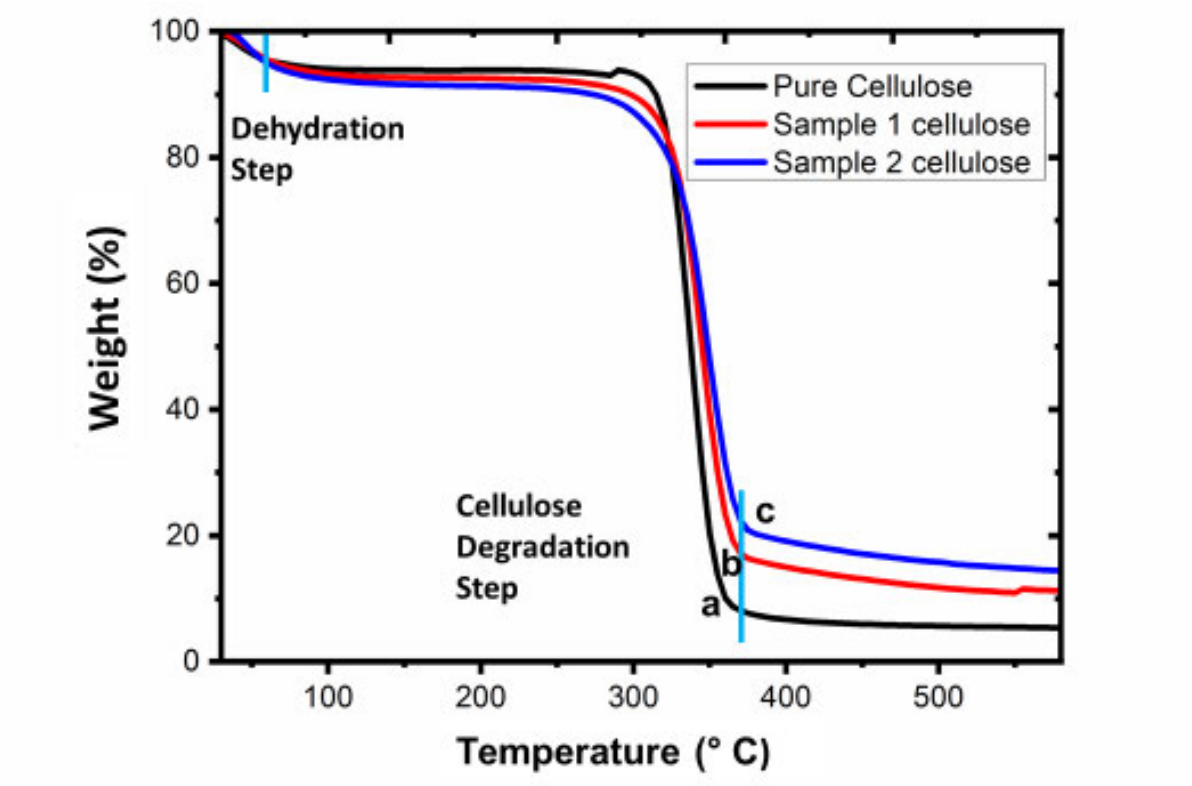

Figure 4.7: TGA of commercial cellulose (a), cellulose sample 1 (b), and cellulose sample 2 (c).

In **Figure 4.7a** the commercial cellulose showed an initial mass loss at 65˚C. This mass loss is attributed to the removal of weakly bonded water molecules and volatile organic materials (Lakshmi et al., 2017). The mass loss between 300 – 360 ˚C approximately 95 % mass change was due to the thermal degradation of the cellulosic materials (Shankar and Rhim et al., 2017). The bonds that are broken are for the hydroxyl and methyl hydroxyl groups present in the cellulose (Lakshmi et al., 2017). The graph stabilizes between the 500 – 600 ˚C and the remaining material (5%) was the char.

The stabilized mass at these higher temperatures was also observed by Mashego et al. (2016) for microcrystalline cellulose (MCC) extracted from sugarcane bagasse.

The thermogram for cellulose sample 1 showed a similar degradation trend (**Figure 4.7b**). The thermogram showed an initial mass loss of weakly bonded moisture content is removed at 55˚C followed by the decomposition of cellulosic materials at approximately 300 ˚C. The thermogram shows a residual char mass of 10 % at 600 ˚C.

The thermogram for the degradation of cellulose sample 2 is shown in **Figure 4.7c** and is similar to that observed for cellulose sample 1 (**Figure 4.7b**) The thermal degradation of commercial cellulose sample 2 begins at 300 ˚C and ends at 380 ˚C. The sample decreased to a weight loss of approximately 14 % indicating a 86 % sample degradation. Cellulose sample 2 showed the lowest mass loss for cellulose degradation. This indicated that cellulose from sugarcane bagasse is thermally more stable at higher temperatures. Joonobi et al. (2010) observed similar degradation patterns for cellulose isolated from bask fibres Leal et al. (2015) also reported that the char remains were carbonaceous residues as a result of intense heating.

4.4.2 Carboxymethyl cellulose

The TGA thermograms in **Figure 4.8** shows the TGA curves of commercial CMC (a), 20 % NaOH CMC (b), 25 % NaOH CMC from cellulose sample 1 (i), 25 % NaOH CMC from cellulose sample 2 and 30 % NaOH CMC (e).

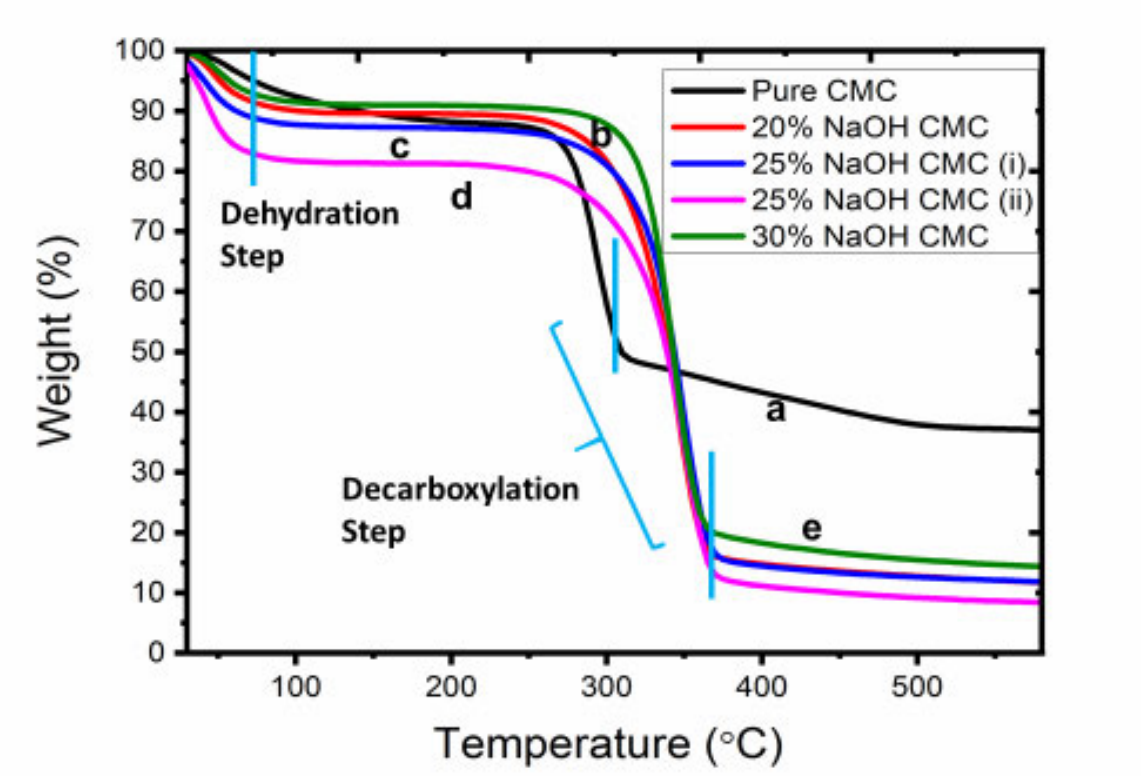

Figure 4.8: TGA of commercial CMC (a), 20 % NaOH CMC (b), 25 % NaOH CMC from cellulose sample 1 (i), 25 % NaOH CMC from cellulose sample 2 and 30 % NaOH CMC (e).

The TGA endotherm (**Figure 4.8a**) showed that commercial CMC has a higher weight percentage at the end of the analysis, which is approximately 37 % of the initial mass. This makes it the most stable of all the samples analysed and this is due to the sodium carboxymethyl substituent from the monochloroacetic acid (MCA) and sodium hydroxide (NaOH). The higher residue for commercial CMC can be attributed to the industrial preparation method of the CMC, its higher recalcitrant nature, its higher purity and the source of the carbon-based raw material used for the commercial CMC preparation being different to the biodegradable CMC from sugarcane bagasse. CMCs have also been reported to be more thermally stable materials than cellulose (Sun

et al., 2004). The thermogram in **Figure 4.8a** also shows an initial mass loss from 45˚C to 65˚C. This mass loss is attributed to absorbed moisture and volatile organic solvents. A significant mass loss is observed at the 280 – 300˚C temperature range, this is the decarboxylation of the COO^- bond and the loss of CO_2. The mass loss is observed over a small temperature range while a 40% mass loss is observed in this region, complete degradation of the sample was observed at around 500 ˚C. Thereafter, a constant mass can be observed.

Figure 4.8b showed the degradation pattern of 20% NaOH CMC had an initial mass loss at 55˚C. This was attributed to the loss of volatile moisture content. At 270˚C, a mass change that is very significant was observed that was over a larger range till 370˚C is attributed to decarboxylation which results in the large weight percentage decrease. The mass % stays constant beyond 500˚C.

In **Figures 4.8b** – **c** for 20% NaOH CMC and 25% NaOH from cellulose sample 1 showed similar degradation patterns. The CMC sample with the highest NaOH wt. % loading had the highest thermal stability, which could elude to commercial CMC being industrially prepared at higher NaOH wt. %. Golbaghi et al. (2017) used approximately 40 % NaOH (w/v) at higher MCA wt. % loading and had a more thermally stable product with 40 % char.

4.2.4 Differential scanning calorimetry (DSC)

4.2.4.1 Cellulose

The DSC thermograms for all cellulose and CMC samples are represented as endothermic peaks as shown in **Figure 4.9**. The DSC in **Figure 4.9** below shows the endotherm for commercial cellulose (a), cellulose sample 1 (b) and cellulose sample 2 (c).

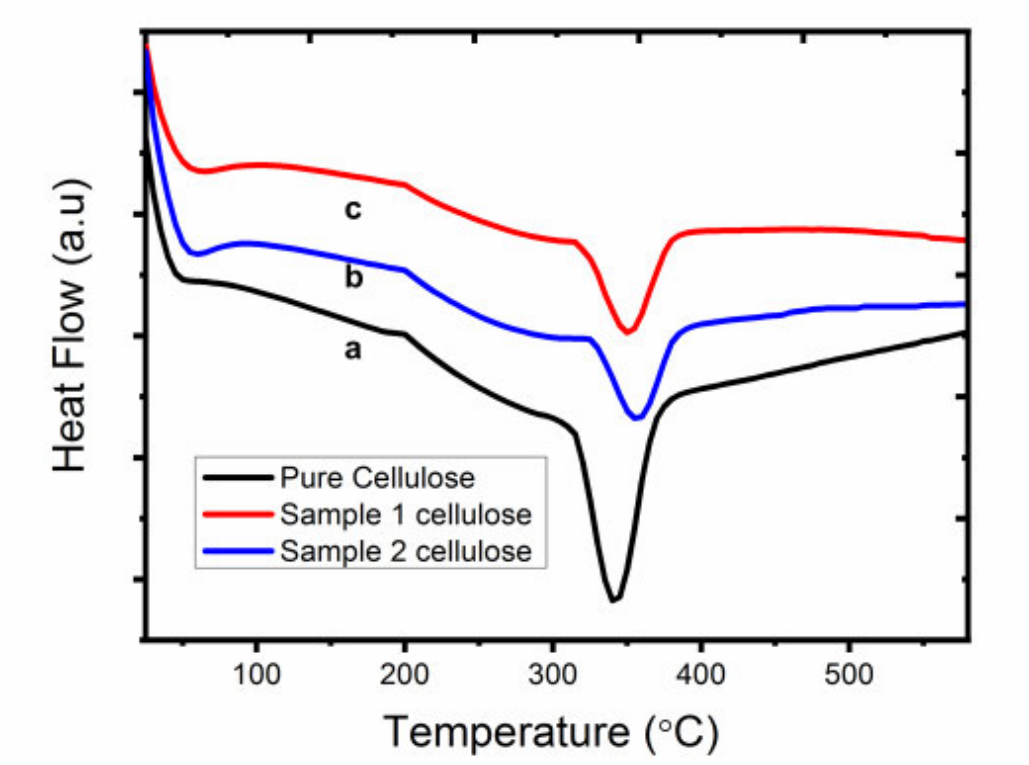

Figure 4.9: DSC endotherm of commercial cellulose (a), cellulose sample 1 (b) and cellulose sample 2 (c).

The DSC for pure cellulose is seen in **Figure 4.9a**. It is represented by the smooth peak on the left shoulder in the low temperature region accompanied by a small peak that was attributed to moisture loss (Yang et al., 2007). The second region, which is a sharp peak at the maximum decomposition rate at 345˚C is attributed to cellulose decomposition. The onset temperature for residual materials decomposition in the cellulose sample 1 and 2 shown in **Figure 4.9b** – **c** are 255 and 265˚C, respectively. Both possess the smooth peak on the left shoulder and the sharp

peak similar to commercial cellulose. The endotherm curves shown in **Figure 4.10** are consistent with those found by Morán et al. (2008). Commercial cellulose shows the most intense peak at the lowest observed temperature, which suggests that the rate of depolymerisation occurs more rapidly for the commercial sample. Cellulose sample 1 and 2 are slightly more thermally stable than commercial cellulose and show evidence of stronger interaction or hydrogen bonding (Kian et al. 2017).

4.2.4.1 Carboxymethyl cellulose

Figure 4.10 shows the DSC endotherms of the commercial CMC (a), 20 wt. % NaOH CMC (b) 25 wt. % NaOH CMC from cellulose sample 1 (c), 25 wt. % NaOH CMC from cellulose sample 2 (d) and 30 wt. % NaOH CMC (e).

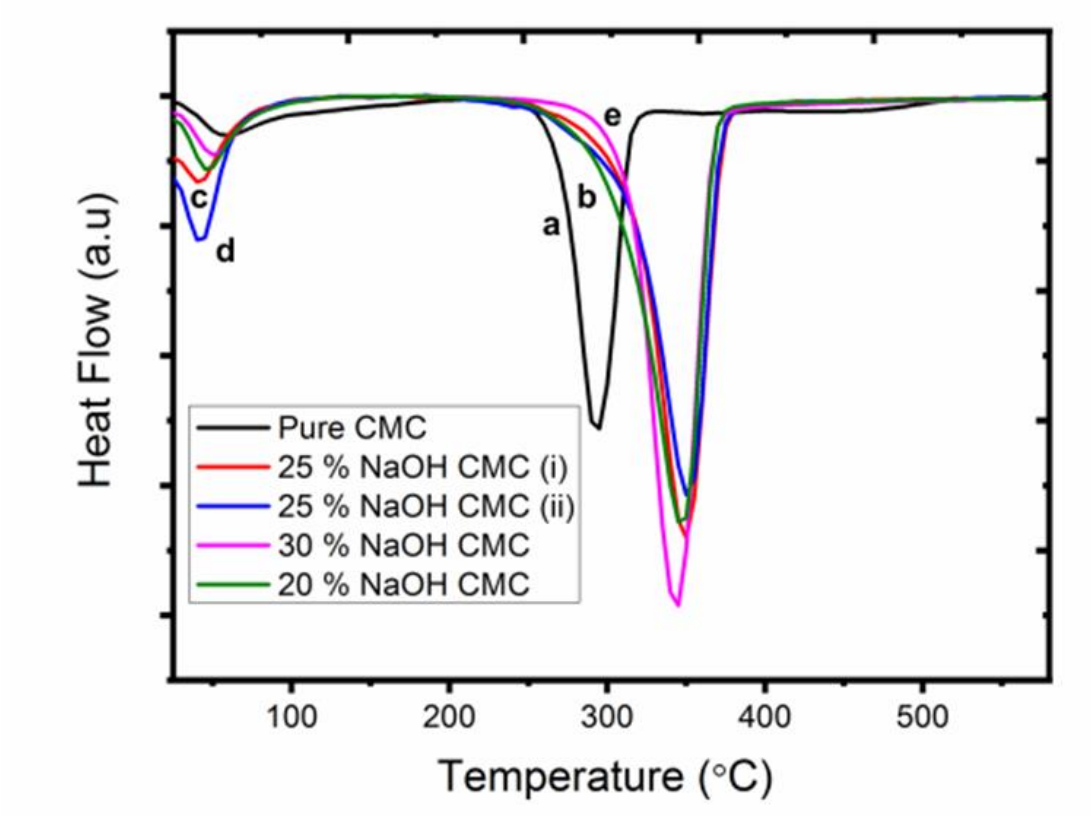

Figure 4.10: DSC endotherm of the commercial CMC (a), 20 wt. % NaOH CMC (b) 25 wt. % NaOH CMC from cellulose sample 1 (c), 25 wt. % NaOH CMC from cellulose sample 2 (d) and 30 wt. % NaOH CMC (e).

.

Figure 4.10 showed two main peaks where the first peak is assigned to water evolution at < 100 ˚C. In CMC, the presence of hydroxyl and carboxylate anions increase moisture adsorption. The second peak at approximately 300 °C and 350 ˚C for the commercial and synthesised CMCs respectively, is for the breaking of the carboxymethyl group (-CH_2COONa) and the release CO_2 from CMCs (Koh, 2013; Casaburi et al., 2017). The synthesized samples showed more well-defined peaks at 50 ˚C, 55 ˚C, 50 ˚C and 50 ˚C for 20 %, 25 % (i), 25% (ii) and 30% NaOH CMC, respectively. These peaks were more pronounced than for commercial CMC, indicating that more moisture could be absorbed on the surface of the synthesised CMC product.

The second peak of the commercial CMC endotherm at 295˚C is the maximum decomposition temperature. The maximum decomposition temperatures at 345 ˚C, 350˚C, 350˚C, and 350 ˚C were observed for 20%, 25% (i), 25% (ii) and 30% NaOH CMC, respectively. The NaOH concentration can be attributed to the higher temperature degradation patterns as was also observed by Rosnah et al. (2006). The degree of substitution due to higher NaOH wt. % concentrations (Schlufter and Heinze et al. 2010) also affects the degradation temperature due to shifts in the polymer arrangement. Casaburi et al. (2017) investigated the effects of DS on CMC from bacterial cellulose and similarly observed that samples with a varying DS will have different decomposition temperatures even if the variance is marginal.

4.2.5 Scanning electron microscopy (SEM)

4.2.5.1 Cellulose

Scanning electron microscopy (SEM) images for commercial cellulose (a), cellulose sample 1 (b) and cellulose sample 2 (c) samples are shown on **Figure 4.11**.

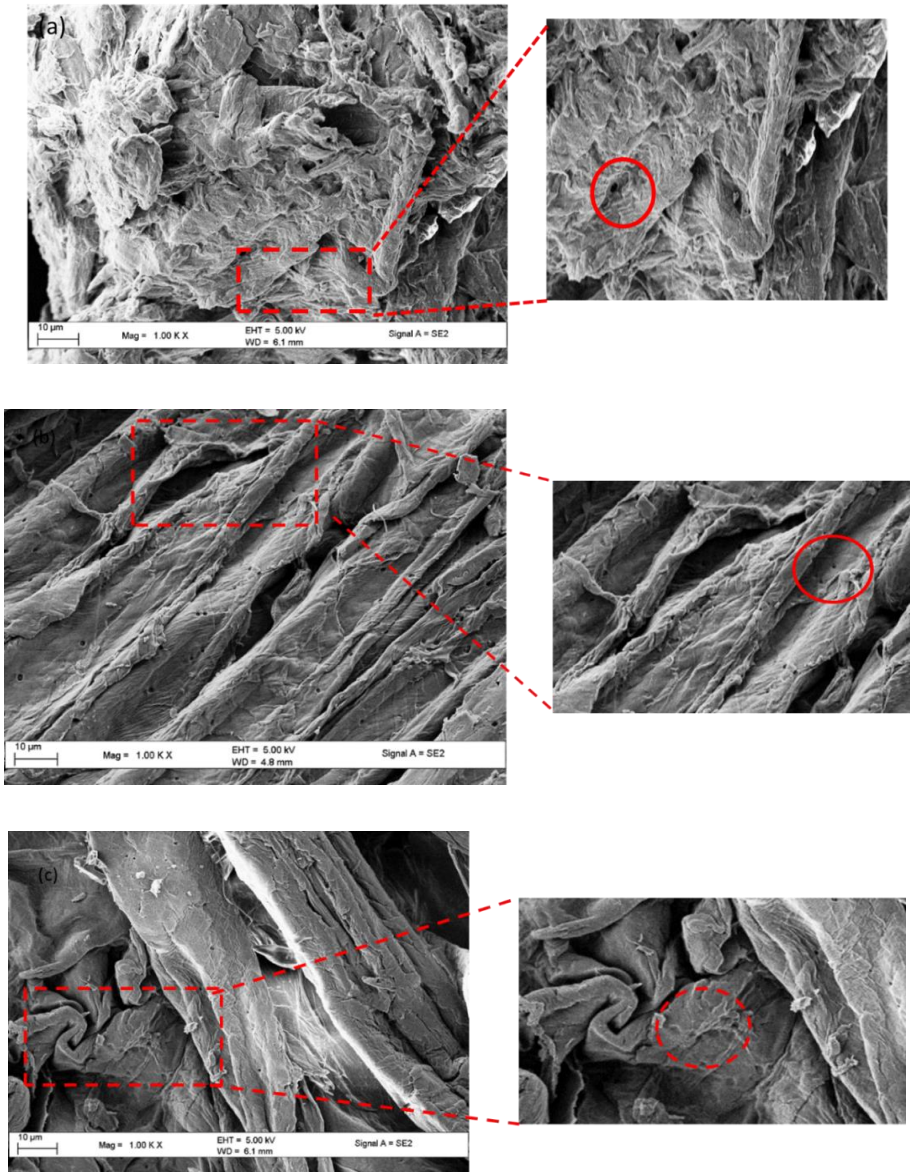

Figure 4.11: SEM images for commercial cellulose (a), cellulose sample 1 (b) and cellulose sample 2 (c)**.**

The SEM images in **Figure 4.11** are consistent with images obtained by Shankar et al. (2017) at 200 µm magnification range. The SEM image of pure cellulose in **Figure 4.11a** shows a rough surface exterior that has an irregular morphology. Cellulose formed intertwined bundles and these bundles form a larger clustered matrix network in the range of 20 – 200 nm. This is a result of the presence of the cellulose polymer (Krishnamachari et al. 2011). SEM images in **Figure 4.11c** show the network of fibrils is inter-locked. Cellulose samples 1 and 2 have similar morphologies to commercial cellulose. There are observable similarities between both cellulose samples; however, cellulose sample 1 showed a smoother morphology and an absence of the irregular shapes. All cellulose images also showed a presence of small alveolate holes that have been highlighted and circled in **Figure 4.11** which have also been observed by Li et al. (2010) after pre-treatment of starch isolated from an under-utilized Liliaceae plant which was to be carboxymethylated. Alveolate holes were also seen in native pulp images by Joshi et al. (2015) post pre-treatment.

4.2.5.2 Carboxymethyl cellulose

SEM images for commercial and synthesised CMC samples are shown in **Figures 4.12** – **4.16**. **Figures 4.12** – **4.16** are for commercial CMC, 20 wt. % NaOH CMC, 25 wt. % NaOH CMC from cellulose sample 1, 25 wt. % NaOH CMC from cellulose sample 2 and 30 wt. % NaOH CMC, respectively at varying magnifications (290 – 500 x magnifications).

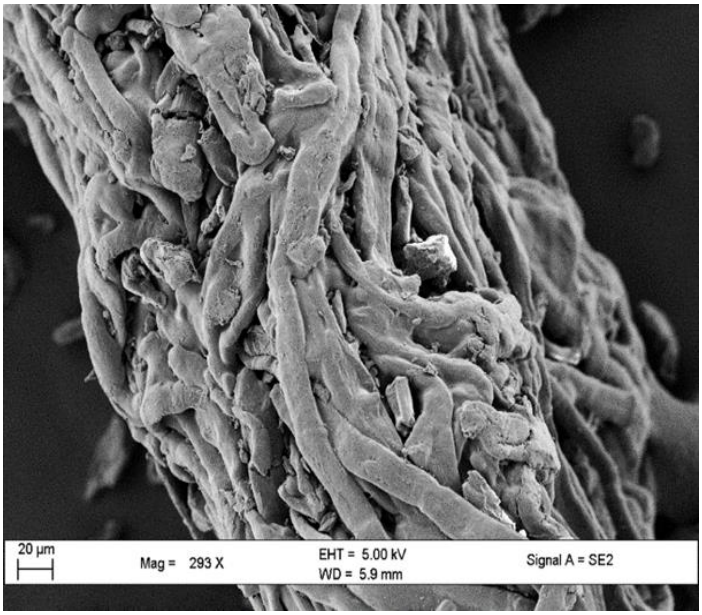

Figure 4.12: SEM of commercial CMC

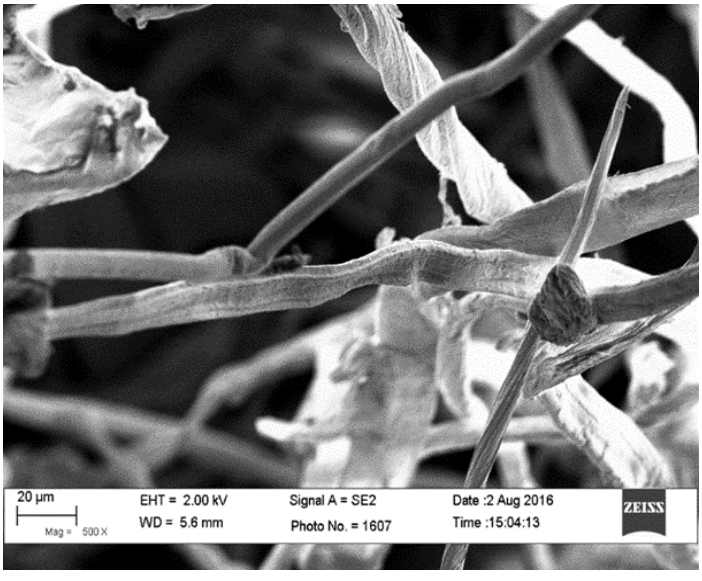

Figure 4.13: SEM of 20% NaOH CMC

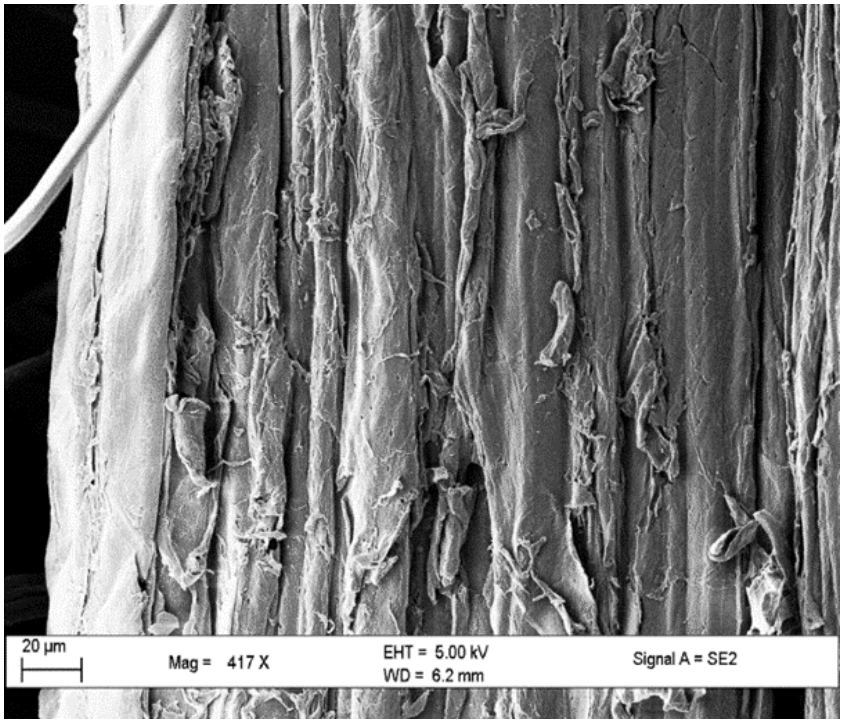

Figure 4.14: SEM of 25 % NaOH CMC from cellulose sample 1

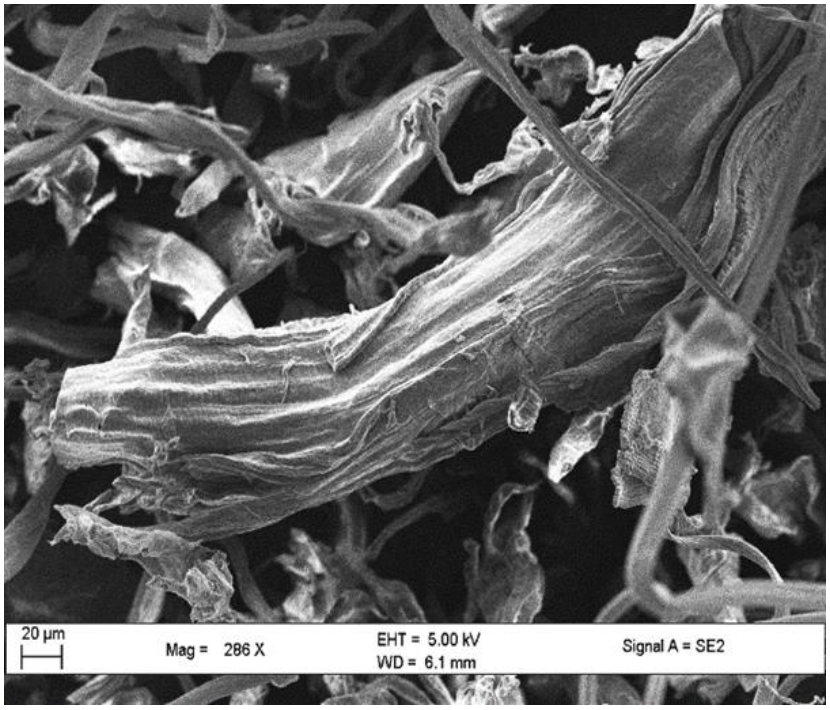

Figure 4.15: SEM of 25 % NaOH CMC from cellulose sample 2

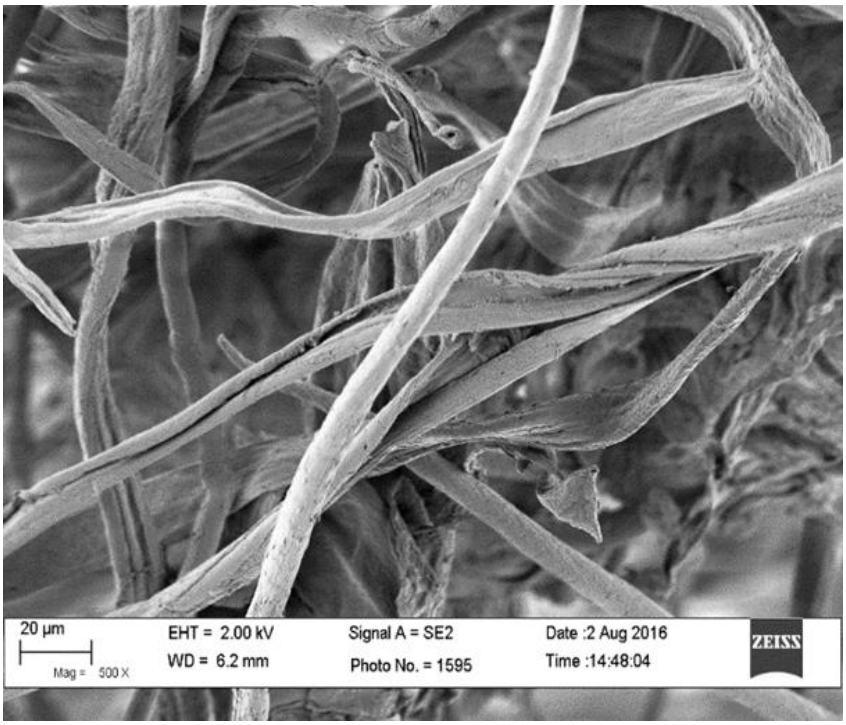

Figure 4.16: SEM image of 30 % NaOH CMC

Each image was calibrated at 20 µm. The synthesised CMC samples (**Figure 4.11**- **Figure 4.16**) showed a contrast to the commercial cellulose images: the CMC fibres are now smoother and showed finer surface textures at varying NaOH concentrations. The fibres at the 30 % NaOH concentration are well defined with defined with no bundling Sutka et al. (2015) reported similar fibrils are for **Figure 4.12**, **Figure 4.14** and **Figure 4.15**. The CMC fibrils are elongated for commercial, 20 % and 30 % NaOH CMCs. The CMC fibrils are intertwined for 25 % NaOH CMCs (**Figure 4.11** and **4.12**) and showed bundles of fibres that are not well separated into individual fibrils similar to that by Abdel-Halim et al. (2015).

The surface morphologies are shown in **Figure 4.17** for commercial CMC (a), 20 % NaOH CMC,25 % NaOH CMC from cellulose sample 1 (c), 25 % NaOH CMC from cellulose sample 2 (d) and 30 % NaOH CMC. These images are at higher magnifications (2500 – 9000 x magnification) at a calibrated length of 2 µm.

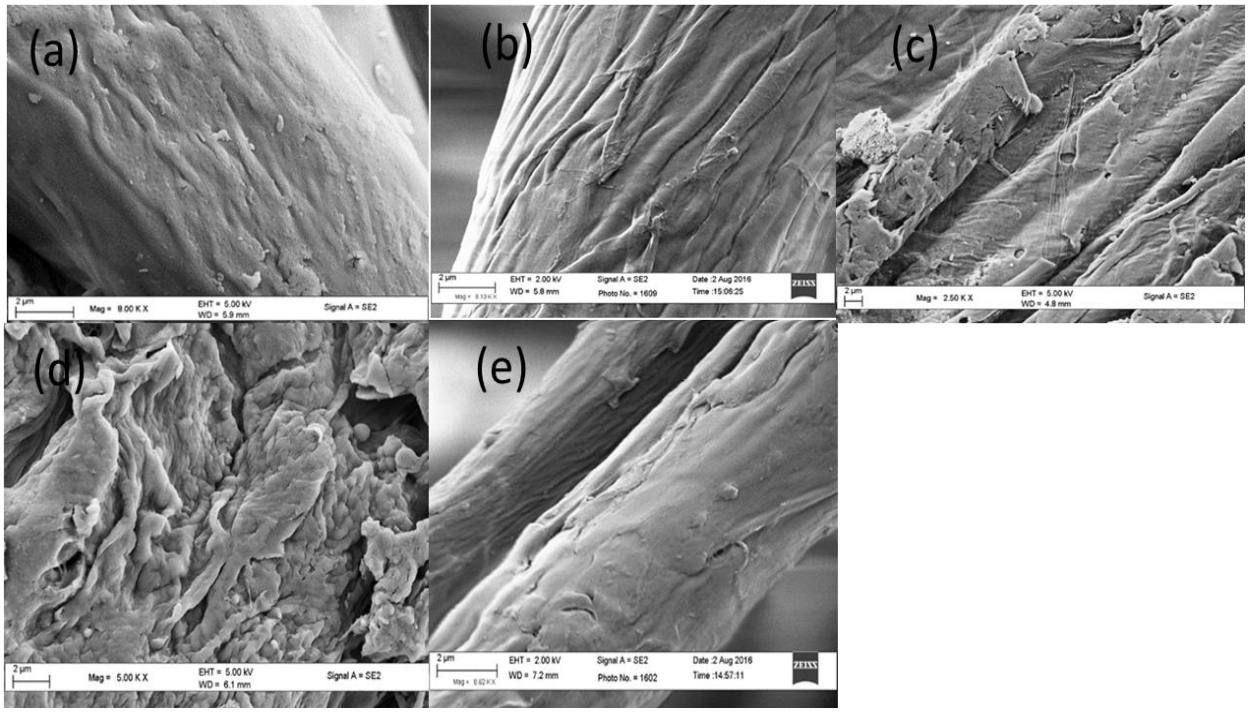

Figure 4.17: SEM image of all CMC samples

At higher resolutions **Figures 4.17 (a)**, **(b)** and **(d)** showed a smooth surface morphology similar to that reported by Heydarzadeh et al. (2009). **Figure 4.17 (c)** and **(d)** shows a rougher surface when compared to **Figures 4.12** – **4.14**. But the bundles or intertwining of the fibres are clearly evident. The images for the 25 % NaOH CMCs showed deep methylation and etherification which is consistent with that observed by Heydarzadeh et al. (2009) and Candido et al. (2016).

4.2.6 Transmission electron microscopy (TEM)

4.2.6.1 Cellulose

Figure 4.18 are the TEM images of commercial cellulose (a,b), cellulose sample 1 (c,d) and cellulose sample 2 (e,f).

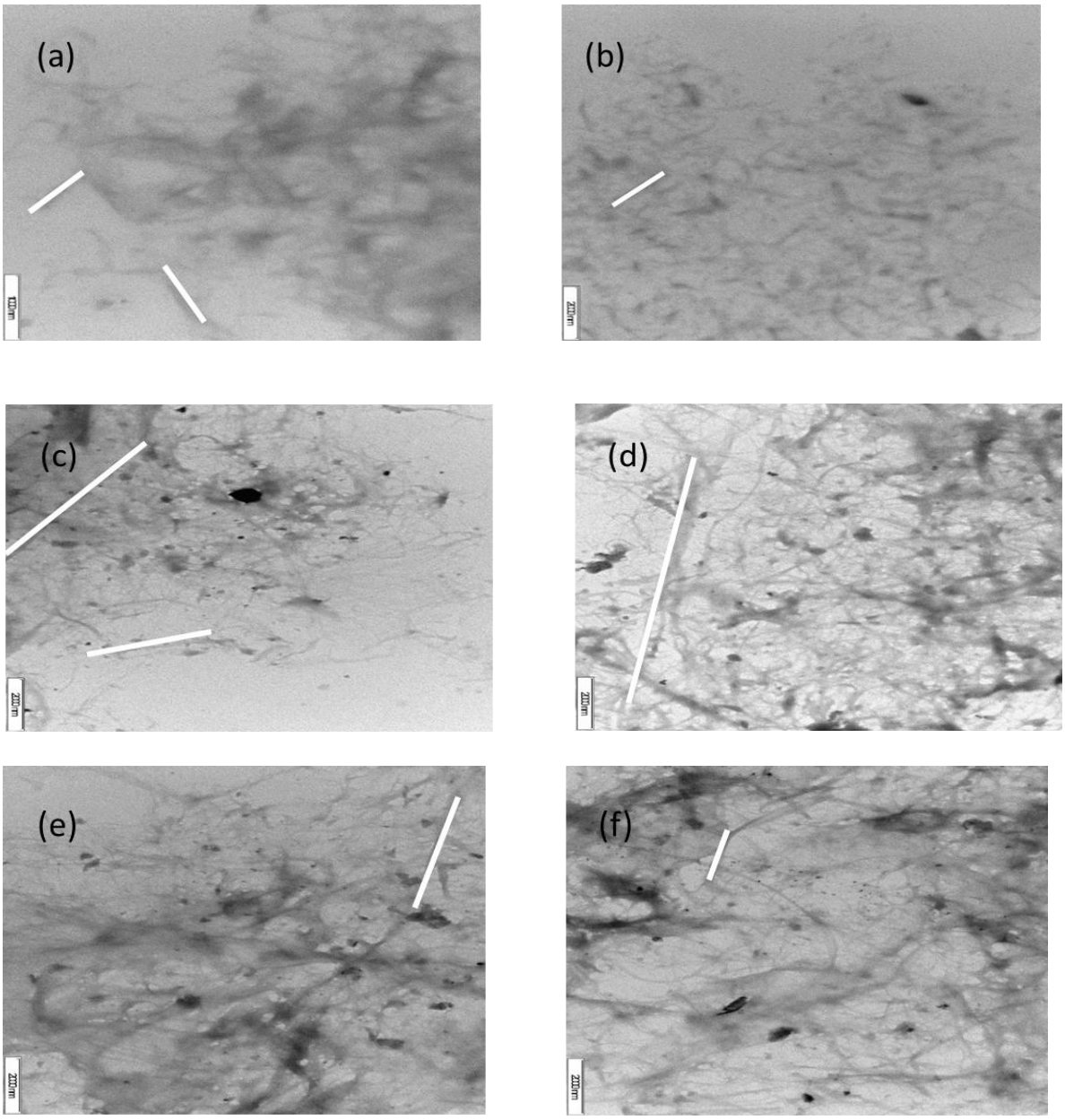

Figure 4.18: TEM images of commercial cellulose (a,b), cellulose sample 1 (c,d) and cellulose sample 2 (e,f).

The images on **Figure 4**.**18** show calibration of 2000 nm with the exception for **Figure 4**.**18a** which is 1000 nm. All samples showed fibrils that are common for cellulosic materials. The length of the commercial cellulose fibrils was approximately 200 nm as seen on **Figure 4**.**18a** - **b** while cellulose samples 1 and 2 show much longer fibrils (approx. 600 nm) similar to that reported by Krishnamachari et al. (2011). The agglomeration of fibrils all extracted cellulose are consistent with literature findings observed by Malainine, (2005) and Peterson et al. (2006). The cellulose sample 2 showed entangled fibres (Deepa et al., 2015) which are consistent with the SEM images. The alveolate are also visible in the TEM images.

.

4.2.6.2 Carboxymethyl cellulose

Figure 4.19 shows the TEM images of commercial CMC (a), 20 wt. % NaOH CMC (b) 25 wt. % NaOH CMC from cellulose sample 1 (c), 25 wt. % NaOH CMC from cellulose sample 2 (d) and 30 wt. % NaOH CMC (e).

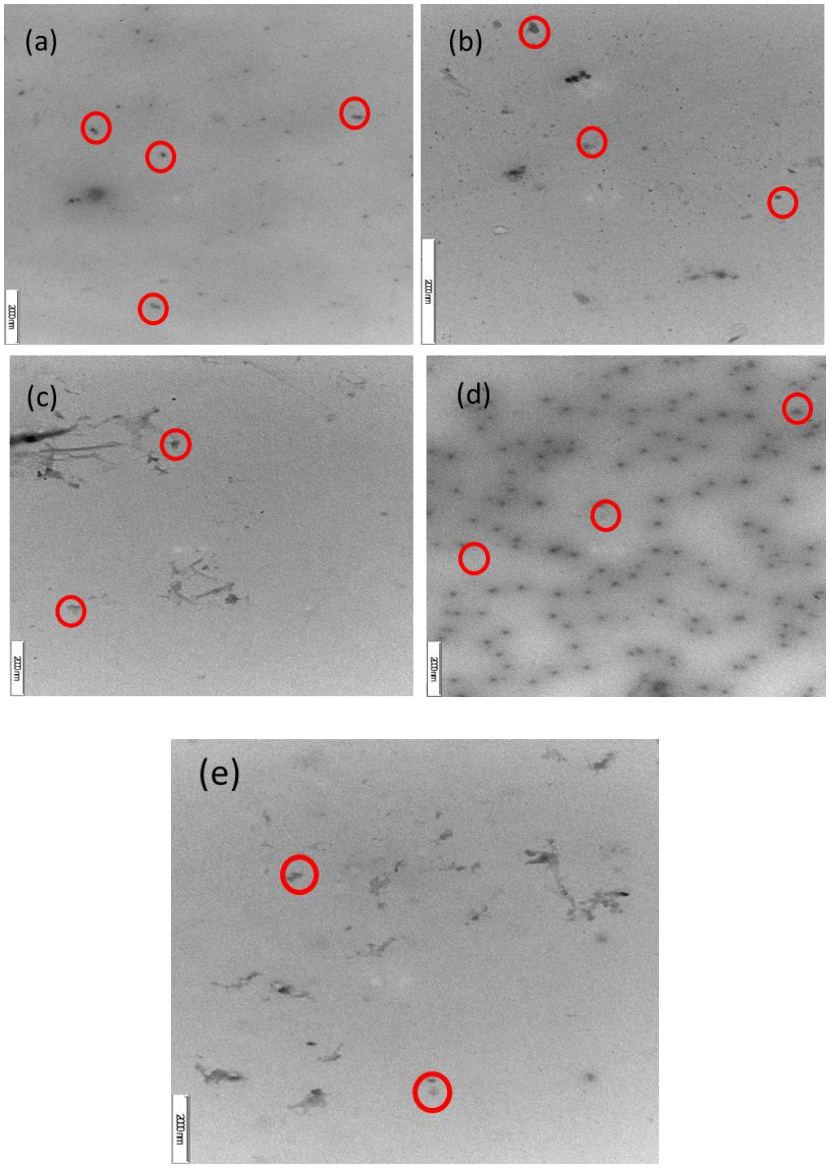

Figure 4.19: TEM images commercial CMC (a), 20 wt. % NaOH CMC (b) 25 wt. % NaOH CMC from cellulose sample 1 (c), 25 wt. % NaOH CMC from cellulose sample 2 (d) and 30 wt. % NaOH CMC (e).

TEM images in **Figure 4.19** are contrast to those seen in **Figure 4.18**. The TEM images indicate that the synthesised CMCs have a different shape and size. The CMC particles are the dark spherical spots (Hashem et al. 2013). Hashem et al. (2013) reported TEM images of CMC hydrogels that showed similar characteristic dark spheres. Composite CMC materials were reported by Salama et al. (2016) and showed similar shape and rheology to **Figure 4.18**. The synthesised CMC particles had an average length of a few nanometres (5 -25 nm). CMC aerogel composites studied by Yu et al. (2017) showed particle length size of ±10 nm similar to this work.

4.2.7 Degree of substitution (DS)

Equation 3.3 was used to calculate the DS value. A sample calculation of DS value is shown below:

$$DS = \frac{0.162\left(\frac{0.1\,b}{G}\right)}{1-0.080\left(\frac{.0.01\,b}{G}\right)} = \frac{0.162\left(\frac{0.1\,(2.20)}{0.1015}\right)}{1-0.080\left(\frac{.0.01\,(2.20)}{0.1015}\right)} = 0.3573$$

Table 4.4 lists the DS values for all the commercial and synthesised CMC samples.

Table 4.4: Average DS values of all CMC samples.

CMC sample	**Mass of CMC powder g/(G)**	**Volume of titration (b)/ml**	**DS**
Pure CMC	0.1095	2.60	0.42
20% NaOH CMC	0.1015	2.20	0.36
25% NaOH CMC (i)	0.1027	2.30	0.37
25% NaOH CMC (ii)	0.1055	2.25	0.37
30% NaOH CMC	0.1194	2.60	0.42

The highest DS value (0.42) was obtained from the synthesised 30 % NaOH CMC product (**Table 4.4)**. is a DS = 0.42 this was obtained with 30 % NaOH (w/w) where the CMC was synthesised with a mass of 1.2 g of monochloroacetic acid (MCA). The CMC was produced from cellulose sample 1. There is an increase in DS values from 0.357, 0.366 and 0.420 with an increase in NaOH concentrations: 20, 25, and 30 % (w/v) NaOH CMC, respectively. In literature dos Santos et al. (2015) reported a DS of 1.46 where 5 g of MCA was reacted for every gram of cellulose extracted from brewers spent grain (BSG).The solvent that was used in this study gave the highest DS in a study done by Pushpamalar et al. (2006) but different solvent: water ratios were reported to also used to optimize the DS value. Golbaghi et al. (2017) attributed higher DS to increased NaOH wt. % loading at higher reaction temperatures with prolonged reaction times**.**

CHAPTER FIVE

CONCLUSIONS AND RECOMMENDATIONS

5.1 Conclusions

Cellulose was extracted by delignification of SCB in 8 M and 4 M HNO_3 solutions. XRD analysis of the extracted and commercial cellulose samples showed the presence of cellulose I and II. The imaging on the TEM and SEM showed that cellulose fibrils. SEM at higher resolution showed similar surface morphology in all cellulose samples. Higher nitric acid concentration showed cellulose surface was smoother.

CMC XRD data showed that there is a single peak characteristic of carboxymethyl functional group which was also confirmed by the FTIR analysis. SEM and TEM images showed the dark spots characterized by commercial CMC. The DS which is another way to characterize CMC was indicated that cellulose at higher NaOH wt. % loading has a similar DS with commercial CMC. All the characterization that was done on the samples confirms successful delignification and subsequent carboxymethylation.

5.2 Recommendations

Sugarcane bagasse shows great promise as a source of cellulose, alternate pre-treatment methods can also be investigated, and their relative properties characterized. The use of a batch reactor (Parr reactor) to conduct experiments at elevated conditions to improve product quality could be assessed using a number of parameter variations in a Box-Behnken design of experiments. CMC production from other biomass sources could also be a viable study for investigation. The further optimization of different sources for the alkaline process such as potassium hydroxide (KOH) would also yield results of interest.

REFERENCES

Abdel-Halim, E.S., Alanazi, H.H. and Al-Deyab, S.S., 2015. Utilization of olive tree branch cellulose in synthesis of hydroxypropyl carboxymethyl cellulose. *Carbohydrate Polymers*, *127*, pp.124-134.

Abouloula, C.N., Rizwan, M., Selvanathan, V., Abdullah, C.I., Hassan, A., Yahya, R. and Oueriagli, A., 2018. A novel application for oil palm empty fruit bunch: extraction and modification of cellulose for solid polymer electrolyte. *Ionics*, *24*(12), pp.3827-3836.

Adinugraha, M.P. and Marseno, D.W., 2005. Synthesis and characterization of sodium carboxymethylcellulose from cavendish banana pseudo stem (Musa cavendishii LAMBERT). *Carbohydrate Polymers*, *62*(2), pp.164-169.

Adinugraha, M.P. and Marseno, D.W., 2005. Synthesis and characterization of sodium carboxymethylcellulose from cavendish banana pseudo stem (Musa cavendishii LAMBERT). *Carbohydrate Polymers*, *62*(2), pp.164-169.

Aguir, C. and M'Henni, M.F., 2006. Experimental study on carboxymethylation of cellulose extracted from Posidonia oceanica. *Journal of Applied Polymer Science*, *99*(4), pp.1808-1816.

Alberts, B., Johnson, A., Lewis, J., Raff, M., Roberts, K. and Walter, P., 2002. Cell junctions. In *Molecular Biology of the Cell. 4th edition*. Garland Science.

Aliouche, D., Bal, K.E. and Lahfati, K., 2000, November. Cinetique d'absorption des liquides par les biotextiles a structure absorbante complexe. Influence des gels de polymeres superabsorbants. In *Annales de Chimie Science des Matériaux* , 25(7) pp. 557-566).

Almasi, H., Ghanbarzadeh, B. and Entezami, A.A., 2010. Physicochemical properties of starch–CMC–nanoclay biodegradable films. *International Journal of Biological Macromolecules*, *46*(1), pp.1-5.

Ambjörnsson, H.A., Schenzel, K. and Germgård, U., 2013. Carboxymethyl cellulose produced at different mercerization conditions and characterized by NIR FT Raman spectroscopy in combination with multivariate analytical methods. *BioResources*, *8*(2), pp.1918-1932.

Balat, M., 2011. Production of bioethanol from lignocellulosic materials via the biochemical pathway: a review. *Energy Conversion and Management*, *52*(2), pp.858-875.

Balser K, Hoppe L, Eicher T, Wandel M, Astheimer HJ, Steinmeier H, Allen JM (1986) Cellulose esters. In: Gerhartz W, Stephen YY, Thomas CF, Pfefferkorn R, James F (eds) Ullmann's Encyclopedia of Industrial Chemistry. Wiley, New York.

Balser, K., 1986. Cellulose Esters, Ullmann s Encyclopedia of Industrial Chemistry, vol. A5, Ed. E. Gerhartz[b].

Banda, A., 2002. *Electricity production from sugar industries in Africa: A case of South Africa* (Doctoral dissertation, University of Cape Town, Cape Town, South Africa).

Barai, B.K., Singhal, R.S. and Kulkarni, P.R., 1997. Optimization of a process for preparing carboxymethyl cellulose from water hyacinth (Eichornia crassipes). *Carbohydrate Polymers*, *32*(3-4), pp.229-231.

Barakat, A., Mayer-Laigle, C., Solhy, A., Arancon, R.A., De Vries, H. and Luque, R., 2014. Mechanical pretreatments of lignocellulosic biomass: towards facile and environmentally sound technologies for biofuels production. *RSC Advances*, 4(89), pp.48109-48127.

Batdorf, J.B. and Rossman, J.M., 1973. Sodium carboxymethylcellulose. In *Industrial Gums* (pp. 695-729). Academic Press.

Batelaan, J.G, Van Ginkel C.G, and Balk F. (1992). Carboxymethylcellulose (CMC). *The Handbook of Environmental Chemistry*. 3(1), pp.329-335.

Bezerra, T.L. and Ragauskas, A.J., 2016. A review of sugarcane bagasse for second-generation bioethanol and biopower production. *Biofuels, Bioproducts and Biorefining*, *10*(5), pp.634-647.

Bibi, S., Bremner, D.H., Macdougall-Heasman, M., Reid, R., Simpson, K., Tough, A., Waddell, S., Stewart, I.J. and Matthews, K.H., 2015. A preliminary investigation to group disparate batches of licit and illicit diazepam tablets using differential scanning calorimetry. *Analytical Methods*, *7*(20), pp.8597-8604.

Bilal, M., Asgher, M., Iqbal, H.M., Hu, H. and Zhang, X., 2017. Biotransformation of lignocellulosic materials into value-added products—a review. *International Journal of Biological Macromolecules*, 98, pp.447-458.

Binod, P., Satyanagalakshmi, K., Sindhu, R., Janu, K.U., Sukumaran, R.K. and Pandey, A., 2012. Short duration microwave assisted pretreatment enhances the enzymatic saccharification and fermentable sugar yield from sugarcane bagasse. *Renewable Energy*, *37*(1), pp.109-116.

Bono, A., Ying, P.H., Yan, F.Y., Muei, C.L., Sarbatly, R. and Krishnaiah, D., 2009. Synthesis and characterization of carboxymethyl cellulose from palm kernel cake. *Advances in Natural and Applied Sciences*, *3*(1), pp.5-12.

Broido, A., 1969. A simple, sensitive graphical method of treating thermogravimetric analysis data. *Journal of Polymer Science Part A-2: Polymer Physics*, *7*(10), pp.1761-1773.

Candido, R.G. and Gonçalves, A.R., 2016. Synthesis of cellulose acetate and carboxymethylcellulose from sugarcane straw. *Carbohydrate Polymers*, *152*, pp.679-686.

Carrere, H., Antonopoulou, G., Affes, R., Passos, F., Battimelli, A., Lyberatos, G. and Ferrer, I., 2016. Review of feedstock pretreatment strategies for improved anaerobic digestion: from lab-scale research to full-scale application. *Bioresource Technology*, *199*, pp.386-397.

Casaburi, A., Rojo, Ú.M., Cerrutti, P., Vázquez, A. and Foresti, M.L., 2018. Carboxymethyl cellulose with tailored degree of substitution obtained from bacterial cellulose. *Food Hydrocolloids*, *75*, pp.147-156.

Casaburi, A., Rojo, Ú.M., Cerrutti, P., Vázquez, A. and Foresti, M.L., 2018. Carboxymethyl cellulose with tailored degree of substitution obtained from bacterial cellulose. *Food Hydrocolloids*, *75*, pp.147-156.

Chambon, C.L., Mkhize, T.Y., Reddy, P., Brandt-Talbot, A., Deenadayalu, N., Fennell, P.S. and Hallett, J.P., 2018. Pretreatment of South African sugarcane bagasse using a low-cost protic ionic liquid: a comparison of whole, depithed, fibrous and pith bagasse fractions. *Biotechnology for Biofuels*, *11*(1), p.247.

Chen, W.H., Ye, S.C. and Sheen, H.K., 2012. Hydrolysis characteristics of sugarcane bagasse pre-treated by dilute acid solution in a microwave irradiation environment. *Applied Energy*, *93*, pp.237-244.

Chen, W.Q. and Lou, D.P., 2014. Synthesis of sodium carboxymethyl cellulose based on pretreated bamboo shaving. In *Advanced Materials Research*, 997, pp.169-172.

Cheng, H.N., Takai, M. and Ekong, E.A., 1999, May. Rheology of carboxymethylcellulose made from bacterial cellulose. In *Macromolecular Symposia* (Vol. 140, No. 1, pp. 145-153). Weinheim, Germany: WILEY-VCH Verlag GmbH & Co. KGaA.

Cui, M., Wang, F.J., Shao, Z.Q., Lu, F.S. and Wang, W.J., 2011. Influence of DS of CMC on morphology and performance of magnetic microcapsules. *Cellulose*, 18(5), p.1265.

Danafloat., 2017. Copper Ores. Available: http://www.danafloat.com/uk/mining_ores/copper (Accessed July 2017).

Deepa, B., Abraham, E., Cordeiro, N., Mozetic, M., Mathew, A.P., Oksman, K., Faria, M., Thomas, S. and Pothan, L.A., 2015. Utilization of various lignocellulosic biomass for the production of nanocellulose: a comparative study. *Cellulose*, *22*(2), pp.1075-1090.

de Menezes, A.J., Pasquini, D., da Silva Curvelo, A.A. and Gandini, A., 2009. Self-reinforced composites obtained by the partial oxypropylation of cellulose fibers. 1. Characterization of the materials obtained with different types of fibers. *Carbohydrate Polymers*, *76*(3), pp.437-442.

de Oliveira, R.L., da Silva Barud, H., de Assunçao, R.M., da Silva Meireles, C., Carvalho, G.O., Rodrigues Filho, G., Messaddeq, Y. and Ribeiro, S.J.L., 2011. Synthesis and characterization of microcrystalline cellulose produced from bacterial cellulose. *Journal of Thermal Analysis and Calorimetry*, *106*(3), pp.703-709.

Doelle, H.W., 1998. Socio-economic microbial process strategies for a sustainable development using environmentally clean technologies: Sagopalm a renewable resource. *Livestock Research for Rural Development*, *10*(1), p.8.

Dolbow, J., Fried, E. and Ji, H., 2005. A numerical strategy for investigating the kinetic response of stimulus-responsive hydrogels. *Computer Methods in Applied Mechanics and Engineering*, *194*(42-44), pp.4447-4480.

dos Santos, D.M., de Lacerda Bukzem, A., Ascheri, D.P.R., Signini, R. and de Aquino, G.L.B., 2015. Microwave-assisted carboxymethylation of cellulose extracted from brewer's spent grain. *Carbohydrate Polymers*, *131*, pp.125-133.

Duncan, T.V., 2011. Applications of nanotechnology in food packaging and food safety: barrier materials, antimicrobials and sensors. *Journal of Colloid and Interface Science*, *363*(1), pp.1-24.

Durso, D.F., Texas A&M University System, 1981. *Process for the preparation of cellulose ether derivatives*. U.S. Patent 4,254,258.

Egerton, R.F., 2005. *Physical Principles of Electron Microscopy* (p. 41). New York: Springer.

Eliza, M.Y., Shahruddin, M., Noormaziah, J. and Rosli, W.W., 2015. Carboxymethyl cellulose (CMC) from oil palm empty fruit bunch (OPEFB) in the new solvent dimethyl sulfoxide (DMSO)/tetrabutylammonium fluoride (TBAF). In *Journal of Physics: Conference Series*, 622(1) p 012026. IOP Publishing.

Ewing, A.V., Clarke, G.S. and Kazarian, S.G., 2014. Stability of indomethacin with relevance to the release from amorphous solid dispersions studied with ATR-FTIR spectroscopic imaging. *European Journal of Pharmaceutical Sciences*, *60*, pp.64-71.

Fengel, D., Wegener, G. and de Gruyter, W., 1989. *Wood: Chemistry, Ultrastructure, Reactions*. Berlin; New York: W.

Fortune Biotech., 2017. CMC for mosquito coil. Available: http://fortunebiotech.en.made-in-china.com/product/dvJxnhrlTYRm/China-CMC-Carboxymethyl-Cellulose-Sodium-for-Mosquito-Coil.html (Accessed June 2017)

Gabbott, P. ed., 2008. *Principles and Applications of Thermal Analysis*. John Wiley & Sons.

Galbe, M. and Zacchi, G., 2002. A review of the production of ethanol from softwood. *Applied Microbiology and Biotechnology*, *59*(6), pp.618-628.

Golbaghi, L., Khamforoush, M. and Hatami, T., 2017. Carboxymethyl cellulose production from sugarcane bagasse with steam explosion pulping: Experimental, modeling, and optimization. *Carbohydrate Polymers*, *174*, pp.780-788.

Gurland, J. and Tripathi, R.C., 1971. A simple approximation for unbiased estimation of the standard deviation. *The American Statistician*, *25*(4), pp.30-33.

Gupta, B., Agarwal, R. and Sarwar Alam, M., 2013. Preparation and characterization of polyvinyl alcohol-polyethylene oxide-carboxymethyl cellulose blend membranes. *Journal of Applied Polymer Science*, *127*(2), pp.1301-1308.

Gurunathan, T., Mohanty, S. and Nayak, S.K., 2015. A review of the recent developments in biocomposites based on natural fibres and their application perspectives. *Composites Part A: Applied Science and Manufacturing*, *77*, pp.1-25.

Hader, R.N., Waldeck, W.F. and Smith, F.W., 1952. Carboxymethylcellulose. *Industrial & Engineering Chemistry*, *44*(12), pp.2803-2812.

Hansen, T., 2015. CMC Gum. Available: https://digitalfire.com/4sight/material/cmc_gum_228.html (Accessed May 2017).

Hashem, M., Sharaf, S., El-Hady, M.A. and Hebeish, A., 2013. Synthesis and characterization of novel carboxymethylcellulose hydrogels and carboxymethylcellulolse-hydrogel-ZnO-nanocomposites. *Carbohydrate Polymers*, *95*(1), pp.421-427.

He, B.B., Preckwinkel, U. and Smith, K.L., 2000. Fundamentals of two-dimensional X-ray diffraction (XRD2). *Advances in X-ray Analysis*, *43*, pp.273-280.

Heinze, T. and Koschella, A., 2005, March. Carboxymethyl ethers of cellulose and starch–a review. In *Macromolecular Symposia* 223(1) pp. 13-40. Weinheim: WILEY-VCH Verlag.

Heinze, T. and Pfeiffer, K., 1999. Studies on the synthesis and characterization of carboxymethylcellulose. *Die Angewandte Makromolekulare Chemie*, *266*(1), pp.37-45.

Heinze, T., Liebert, T., Klüfers, P. and Meister, F., 1999. Carboxymethylation of cellulose in unconventional media. *Cellulose*, *6*(2), pp.153-165.

Heydarzadeh, H.D., Najafpour, G.D. and Nazari-Moghaddam, A.A., 2009. Catalyst-free conversion of alkali cellulose to fine carboxymethyl cellulose at mild conditions. *World Applied Sciences Journal*, *6*(4), pp.564-569.

Himmel, M.E., Ding, S.Y., Johnson, D.K., Adney, W.S., Nimlos, M.R., Brady, J.W. and Foust, T.D., 2007. Biomass recalcitrance: engineering plants and enzymes for biofuels production. S*cience*, *315*(5813), pp.804-807.

Holst, A., Lask, H. and Kostrzewa, M., Hoechst AG, 1978. *Process for the manufacture of water-absorbing cellulose ethers*. U.S. Patent 4,068,068.

Inkson, B.J., 2016. Scanning electron microscopy (SEM) and transmission electron microscopy (TEM) for materials characterization. In *Materials characterization using nondestructive evaluation (NDE) methods*, pp. 17-43. Woodhead Publishing.

Irochemicals., 2015. Carboxymethyl cellulose oil drilling grade. Available: http://www.irochemical.com/product/Mud-Drilling/CMC.htm (Accessed March 2017).

Joonobi, M., Harun, J., Tahir, P.M., Zaini, L.H., SaifulAzry, S. and Makinejad, M.D., 2010. Characteristic of nanofibers extracted from kenaf core. *BioResources*, *5*(4), pp.2556-2566.

de Jong, E. and Gosselink, R.J., 2014. Lignocellulose-based chemical products. In *Bioenergy Research: Advances and Applications*, pp. 277-313. Elsevier.

Joshi, G., Naithani, S., Varshney, V.K., Bisht, S.S., Rana, V. and Gupta, P.K., 2015. Synthesis and characterization of carboxymethyl cellulose from office wastepaper: A greener approach towards waste management. *Waste Management*, *38*, pp.33-40.

Kamel, S., Ali, N., Jahangir, K., Shah, S.M. and El-Gendy, A.A., 2008. Pharmaceutical significance of cellulose: a review. *Express Polymer Letters*, *2*(11), pp.758-778.

Karataş, M. and Arslan, N., 2016. Flow behaviours of cellulose and carboxymethyl cellulose from grapefruit peel. *Food Hydrocolloids*, *58*, pp.235-245.

Katyal, S., Thambimuthu, K. and Valix, M., 2003. Carbonisation of bagasse in a fixed bed reactor: influence of process variables on char yield and characteristics. *Renewable Energy*, *28*(5), pp.713-725.

Khiari, R., Dridi-Dhaouadi, S., Aguir, C. and Mhenni, M.F., 2010. Experimental evaluation of eco-friendly flocculants prepared from date palm rachis. *Journal of Environmental Sciences*, *22*(10), pp.1539-1543.

Khiari, R., Mhenni, M.F., Belgacem, M.N. and Mauret, E., 2011. Valorisation of vegetal wastes as a source of cellulose and cellulose derivatives. *Journal of Polymers and the Environment*, *19*(1), pp.80-89.

Kian, L.K., Jawaid, M., Ariffin, H. and Alothman, O.Y., 2017. Isolation and characterization of microcrystalline cellulose from roselle fibers. *International Journal of Biological Macromolecules*, 103, pp.931-940.

Klemm, D., Heublein, B., Fink, H.P. and Bohn, A., 2005. Cellulose: fascinating biopolymer and sustainable raw material. *Angewandte Chemie International Edition*, *44*(22), pp.3358-3393.

Koh, M.H., 2013. *Preparation and characterization of carboxymethyl cellulose from sugarcane bagasse* (Masters dissertation, Universiti Tunku Abdul Rahman, Negeri Perak, Malaysia).

Kootstra, A.M.J., Beeftink, H.H., Scott, E.L. and Sanders, J.P., 2009. Comparison of dilute mineral and organic acid pre-treatment for enzymatic hydrolysis of wheat straw. *Biochemical Engineering Journal*, *46*(2), pp.126-131.

Krassig, H. and Schurz, J., 1986. Cellulose. *Ullmann's Encyclopedia of Industrial Chemistry. Weinheim*, Germany: Wiley-VCH.

Krassig, H.A., 1993. Cellulose: Structure, *Accessibilty and Reactivity*.[188].

Kratky, L. and Jirout, T., 2011. Biomass size reduction machines for enhancing biogas production. *Chemical Engineering & Technology*, *34*(3), pp.391-399.

Krishnamachari, P., Hashaikeh, R. and Tiner, M., 2011. Modified cellulose morphologies and its composites; SEM and TEM analysis. *Micron*, 42(8), pp.751-761.

Kulicke, W.M., Kull, A.H., Kull, W., Thielking, H., Engelhardt, J. and Pannek, J.B., 1996. Characterization of aqueous carboxymethylcellulose solutions in terms of their molecular structure and its influence on rheological behaviour. *Polymer*, *37*(13), pp.2723-2731.

Kulicke, W.M., Reinhardt, U., Fuller, G.G. and Arendt, O., 1999. Characterization of the flow properties of sodium carboxymethylcellulose via mechanical and optical techniques. *Rheologica Acta*, *38*(1), pp.26-33.

Ladish, M.R., 1989. Biomass Handbook. In: Kitani, O. and Hall, C.W., (eds). Gordon and Breach Science Publisher: New York. p. 435.

Lakshmi, D.S., Trivedi, N. and Reddy, C.R.K., 2017. Synthesis and characterization of seaweed cellulose derived carboxymethyl cellulose. *Carbohydrate Polymers*, *157*, pp.1604-1610.

Leal, G.F., Ramos, L.A., Barrett, D.H., Curvelo, A.A.S. and Rodella, C.B., 2015. A thermogravimetric analysis (TGA) method to determine the catalytic conversion of cellulose from carbon-supported hydrogenolysis process. *Thermochimica Acta*, 616, pp.9-13.

Lee, S.H., Doherty, T.V., Linhardt, R.J. and Dordick, J.S., 2009. Ionic liquid-mediated selective extraction of lignin from wood leading to enhanced enzymatic cellulose hydrolysis. *Biotechnology and Bioengineering*, *102*(5), pp.1368-1376.

Li, X., Gao, W.Y., Huang, L.J., Wang, Y.L., Huang, L.Q. and Liu, C.X., 2010. Preparation and physicochemical properties of carboxymethyl Fritillaria ussuriensis Maxim. starches. *Carbohydrate Polymers*, *80*(3), pp.768-773.

Limayem, A. and Ricke, S.C., 2012. Lignocellulosic biomass for bioethanol production: current perspectives, potential issues and future prospects. *Progress in Energy and Combustion. Science*, *38*(4), pp.449-467.

Liu, Z.S., Wu, X.L., Kida, K. and Tang, Y.Q., 2012. Corn stover saccharification with concentrated sulfuric acid: effects of saccharification conditions on sugar recovery and by-product generation. *Bioresource Technology*, *119*, pp.224-233.

Lopez, C.G., Rogers, S.E., Colby, R.H., Graham, P. and Cabral, J.T., 2015. Structure of sodium carboxymethyl cellulose aqueous solutions: A SANS and rheology study. *Journal of Polymer Science Part B: Polymer Physics*, *53*(7), pp.492-501.

Lynd, L.R., 1996. Overview and evaluation of fuel ethanol from cellulosic biomass: technology, economics, the environment, and policy. *Annual Review of Energy and the Environment*, *21*(1), pp.403-465.

Ma, H., Zhou, B., Li, H.S., Li, Y.Q. and Ou, S.Y., 2011. Green composite films composed of nanocrystalline cellulose and a cellulose matrix regenerated from functionalized ionic liquid solution. *Carbohydrate Polymers*, *84*(1), pp.383-389.

Malainine, M.E., Mahrouz, M. and Dufresne, A., 2005. Thermoplastic nanocomposites based on cellulose microfibrils from Opuntia ficus-indica parenchyma cell. *Composites Science and Technology*, *65*(10), pp.1520-1526.

Manaf, S.F.A., Jahim, J.M., Harun, S. and Luthfi, A.A.I., 2018. Fractionation of oil palm fronds (OPF) hemicellulose using dilute nitric acid for fermentative production of xylitol. *Industrial Crops and Products*, *115*, pp.6-15.

Mandal, A. and Chakrabarty, D., 2018. Studies on mechanical, thermal, and barrier properties of carboxymethyl cellulose film highly filled with nanocellulose. *Journal of Thermoplastic Composite Materials*, *32*(7), pp.995-1014.

Mann, G., Kunze, J., Loth, F. and Fink, H.P., 1998. Cellulose ethers with a block-like distribution of the substituents by structure-selective derivatization of cellulose. *Polymer*, *39*(14), pp.3155-3165.

Mansouri, S., Khiari, R., Bettaieb, F., El-Gendy, A.A. and Mhenni, F., 2015. Synthesis and characterization of carboxymethyl cellulose from tunisian vine stem: study of water absorption and retention capacities. *Journal of Polymers and the Environment*, *23*(2), pp.190-198.

Marin, F.R., Martha Jr, G.B., Cassman, K.G. and Grassini, P., 2016. Prospects for increasing sugarcane and bioethanol production on existing crop area in Brazil. *BioScience*, *66*(4), pp.307-316.

Martin, C., Klinke, H.B. and Thomsen, A.B., 2007. Wet oxidation as a pre-treatment method for enhancing the enzymatic convertibility of sugarcane bagasse. *Enzyme and Microbial Technology*, *40*(3), pp.426-432.

Mashego, D.V., 2016. *Preparation, isolation and characterization of nanocellulose from sugarcane bagasse* (Masters dissertation, Durban University of Technology, Durban, South Africa).

McGinnis, G.D., Wilson, W.W. and Mullen, C.E., 1983. Biomass pretreatment with water and high-pressure oxygen. The wet-oxidation process. *Industrial & Engineering Chemistry Product Research and Development*, *22*(2), pp.352-357.

Meneses, N.G., Martins, S., Teixeira, J.A. and Mussatto, S.I., 2013. Influence of extraction solvents on the recovery of antioxidant phenolic compounds from brewer's spent grains. *Separation and Purification Technology*, *108*, pp.152-158.

Mesa, L., González, E., Cara, C., González, M., Castro, E. and Mussatto, S.I., 2011. The effect of organosolv pretreatment variables on enzymatic hydrolysis of sugarcane bagasse. *Chemical Engineering Journal*, *168*(3), pp.1157-1162.

Moncada, J., Tamayo, J.A. and Cardona, C.A., 2014. Integrating first, second, and third generation biorefineries: Incorporating microalgae into the sugarcane biorefinery. *Chemical Engineering Science*, *118*, pp.126-140.

Mondal, M.I.H., Yeasmin, M.S. and Rahman, M.S., 2015. Preparation of food grade carboxymethyl cellulose from corn husk agrowaste. *International Journal of Biological Macromolecules*, *79*, pp.144-150.

Monshi, A., Foroughi, M.R. and Monshi, M.R., 2012. Modified Scherrer equation to estimate more accurately nano-crystallite size using XRD. *World Journal of Nano Science and Engineering*, *2*(3), pp.154-160.

Morán, J.I., Alvarez, V.A., Cyras, V.P. and Vázquez, A., 2008. Extraction of cellulose and preparation of nanocellulose from sisal fibers. *Cellulose*, *15*(1), pp.149-159.

Mora-Pale, M., Meli, L., Doherty, T.V., Linhardt, R.J. and Dordick, J.S., 2011. Room temperature ionic liquids as emerging solvents for the pretreatment of lignocellulosic biomass. *Biotechnology and Bioengineering*, *108*(6), pp.1229-1245.

Mussatto, S.I. and Roberto, I.C., 2008. Establishment of the optimum initial xylose concentration and nutritional supplementation of brewer's spent grain hydrolysate for xylitol production by Candida guilliermondii. *Process Biochemistry*, *43*(5), pp.540-546.

Mussatto, S.I., Dragone, G. and Roberto, I.C., 2006. Brewers' spent grain: generation, characteristics and potential applications. *Journal of Cereal Science*, *43*(1), pp.1-14.

Novo, L.P., Gurgel, L.V.A., Marabezi, K. and da Silva Curvelo, A.A., 2011. Delignification of sugarcane bagasse using glycerol–water mixtures to produce pulps for saccharification. *Bioresource Technology*, *102*(21), pp.10040-10046.

Öhgren, K., Vehmaanperä, J., Siika-Aho, M., Galbe, M., Viikari, L. and Zacchi, G., 2007. High temperature enzymatic prehydrolysis prior to simultaneous saccharification and fermentation of steam pretreated corn stover for ethanol production. *Enzyme and Microbial Technology*, *40*(4), pp.607-613.

Olivas, G.I. and Barbosa-Cánovas, G.V., 2005. Edible coatings for fresh-cut fruits. *Critical Reviews in Food Science and Nutrition*, *45*(7-8), pp.657-670.

Padam, B.S., Tin, H.S., Chye, F.Y. and Abdullah, M.I., 2014. Banana by-products: an under-utilized renewable food biomass with great potential. *Journal of Food science and Technology*, *51*(12), pp.3527-3545.

Pecsok, R.L., 1976. Modern Methods of Chemical Analysis. Wiley

Perlack, R.D., 2005. *Biomass as feedstock for a bioenergy and bioproducts industry: the technical feasibility of a billion-ton annual supply*. Oak Ridge National Laboratory. https://nature.berkeley.edu/er100/readings/billion_ton_vision.pdf (Accessed June 2018)

Petersson, L. and Oksman, K., 2006. Biopolymer based nanocomposites: comparing layered silicates and microcrystalline cellulose as nanoreinforcement. *Composites Science and Technology*, *66*(13), pp.2187-2196.

Pires, E.J., Ruiz, H.A., Teixeira, J.A. and Vicente, A.A., 2012. A new approach on brewer's spent grains treatment and potential use as lignocellulosic yeast cells carriers. *Journal of Agricultural and Food Chemistry*, *60*(23), pp.5994-5999.

Ponce, N., Friedman, P. and Leal, D., 1983. Geometric properties and density of bagasse particles. *International Sugar Journal*, *85*(1018), pp.291-295.

Price, D., 2012. Thermogravimetry. Available: https://www.slideshare.net/nimmidalwadi5/tga (Accessed June 2017).

Pushpamalar, V., Langford, S.J., Ahmad, M. and Lim, Y.Y., 2006. Optimization of reaction conditions for preparing carboxymethyl cellulose from sago waste. *Carbohydrate Polymers*, *64*(2), pp.312-318.

Rainey, T.J. and Covey, G., 2016. Pulp and paper production from sugarcane bagasse. *Sugarcane-Based Biofuels and Bioproducts*, pp.1-25.

Rao, M., Industrial utilization of sugar cane and its coproducts. (1997). New Delhi (India) ISPCK Publishers & Distributors.

Rhim, J.W., Park, H.M. and Ha, C.S., 2013. Bio-nanocomposites for food packaging applications. *Progress in Polymer Science*, *38*(10-11), pp.1629-1652.

Rincón, L.E., Becerra, L.A., Moncada, J. and Cardona, C.A., 2014. Techno-economic analysis of the use of fired cogeneration systems based on sugar cane bagasse in south eastern and mid-western regions of Mexico. *Waste and Biomass Valorization*, *5*(2), pp.189-198.

Rodrıguez-Chong, A., Ramírez, J.A., Garrote, G. and Vázquez, M., 2004. Hydrolysis of sugar cane bagasse using nitric acid: a kinetic assessment. *Journal of Food Engineering*, *61*(2), pp.143-152.

Rosnah, M.S., Wan, H., Top, A.M. and Kamarudin, H., 2006. Thermal properties of oil palm fibre, cellulose and its derivatives. *Journal of Oil Palm Research*, pp.272-277.

Rowe, R.C, Sheskey P.J and Quinn M.E. (2013). Handbook of pharmaceutical excipients 7th ed. Pharmaceutical Development and Technology. 18(2) p. 544.

Rowe, R.C., Sheskey, P. and Quinn, M., 2009. *Handbook of pharmaceutical excipients*. Libros Digitales-Pharmaceutical Press.

Salama, A., El-Sakhawy, M. and Kamel, S., 2016. Carboxymethyl cellulose based hybrid material for sustained release of protein drugs. *International Journal of Biological Macromolecules*, *93*, pp.1647-1652.

Sanchez, O.J. and Cardona, C.A., 2008. Trends in biotechnological production of fuel ethanol from different feedstocks. *Bioresource Technology*, *99*(13), pp.5270-5295.

Saputra, A.H., Qadhayna, L. and Pitaloka, A.B., 2014. Synthesis and characterization of carboxymethyl cellulose (CMC) from water hyacinth using ethanol-isobutyl alcohol mixture as the solvents. *International Journal of Chemical Engineering and Applications*, *5*(1), p.36.

Satti, S.A., 2015. *Synthesis and Characterization of Sodium Carboxymethyl Cellulose from the sawdust of Pine wood* (Doctoral dissertation, Sudan University of Science and Technology, Khartoum, Sudan).

Savage, A.B, Young A.E and Maasberg A.T., 1954. Ethers. In: E Ott, H.M Spurling and M.W Grafflin (eds). *Cellulose and cellulose derivatives* Part II. New York: Interscience Publishers, Inc. pp. 882-954.

Schacht, C., Zetzl, C. and Brunner, G., 2008. From plant materials to ethanol by means of supercritical fluid technology. *The Journal of Supercritical Fluids*, *46*(3), pp.299-321.

Schlufter, K. and Heinze, T., 2010, August. Carboxymethylation of bacterial cellulose. In *Macromolecular Symposia* 294(2), pp. 117-124. Weinheim: WILEY-VCH Verlag.

Shankar, S. and Rhim, J.W., 2016. Preparation of nanocellulose from micro-crystalline cellulose: The effect on the performance and properties of agar-based composite films. *Carbohydrate Polymers*, *135*, pp.18-26.

Sidley Chemical[a]. Sodium Carboxymethyl properties. 2015. Available: https://celluloseether.com/properties-of-cmc-carboxymethylcellulose/ (Accessed May 2018)

Sidley Chemical[b]., 2015. Applications of ethers in the paper industry. Available: https://celluloseether.com/carboxymethyl-cellulose-properties-cmc-viscosity/ (Accessed May 2018)

Singh, R.K. and Singh, A.K., 2013. Optimization of reaction conditions for preparing carboxymethyl cellulose from corn cobic agricultural waste. *Waste and Biomass Valorization*, *4*(1), pp.129-137.

SINOCMC. (2011a). The introduction of sodium carboxymethyl cellulose. Available https://www.sino-cmc.com/the-introduction-of-sodium-carboxymethyl-cellulose-cmc/ (Accessed February 2017)

SINOCMC. (2011b). The introduction of sodium carboxymethyl cellulose. Available:http://www.sino-cmc.com/html_news/The-introduction-of-Sodium-Carboxymethyl-Cellulose-4.html (Accessed February 2017)

Skiba, E.A., Budaeva, V.V., Baibakova, O.V., Zolotukhin, V.N. and Sakovich, G.V., 2017. Dilute nitric-acid pretreatment of oat hulls for ethanol production. *Biochemical Engineering Journal*, *126*, pp.118-125.

Soccol, C.R. and Vandenberghe, L.P., 2003. Overview of applied solid-state fermentation in Brazil. *Biochemical Engineering Journal*, *13*(2-3), pp.205-218.

Soykeabkaew, N., Sian, C., Gea, S., Nishino, T. and Peijs, T., 2009. All-cellulose nanocomposites by surface selective dissolution of bacterial cellulose. *Cellulose*, *16*(3), pp.435-444.

Sun, J.X., Sun, X.F., Zhao, H. and Sun, R.C., 2004. Isolation and characterization of cellulose from sugarcane bagasse. *Polymer Degradation and Stability*, *84*(2), pp.331-339.

Sundrop Fuels Inc. (2016). Pretreatment of biomass using steam explosion methods before gasification. Available: https://www.google.com/patents/US20130341569#backward-citations(Accessed February 2017).

Sutka, A., Sutka, A., Gaidukov, S., Timusk, M., Gravitis, J. and Kukle, S., 2015. Enhanced stability of PVA electrospun fibers in water by adding cellulose nanocrystals. *Holzforschung*, *69*(6), pp.737-743.

Talebnia, F., Karakashev, D. and Angelidaki, I., 2010. Production of bioethanol from wheat straw: an overview on pretreatment, hydrolysis and fermentation. *Bioresource Technology*, *101*(13), pp.4744-4753.

Thermo Scientific., 2013. Introduction to Fourier Transform Infrared Spectroscopy. Available:https://tools.thermofisher.com/content/sfs/brochures/BR50555_E_0513M_H_1.pdf (Accessed May 2016).

Tijsen, C.J., Kolk, H.J., Stamhuis, E.J. and Beenackers, A.A.C.M., 2001. An experimental study on the carboxymethylation of granular potato starch in non-aqueous media. *Carbohydrate Polymers*, *45*(3), pp.219-226.

Toğrul, H. and Arslan, N., 2003. Production of carboxymethyl cellulose from sugar beet pulp cellulose and rheological behaviour of carboxymethyl cellulose. *Carbohydrate Polymers*, *54*(1), pp.73-82.

Tomas-Pejo, E., Oliva, J.M. and Ballesteros, M., 2008. Realistic approach for full-scale bioethanol production from lignocellulose: a review. *Journal of Scientific & Industrial Research*, 67, pp.874-884.

Tsapekos, P., Kougias, P.G. and Angelidaki, I., 2018. Mechanical pretreatment for increased biogas production from lignocellulosic biomass; predicting the methane yield from structural plant components. *Waste Management*, *78*, pp.903-910.

Valim, I.C., Fidalgo, J.L., Rego, A.S., Vilani, C., Martins, A.R.F. and Santos, B.F., 2017. Neural network modeling to support an experimental study of the delignification process of sugarcane bagasse after alkaline hydrogen peroxide pre-treatment. *Bioresource Technology*, *243*, pp.760-770.

Varshney, V.K., Gupta, P.K., Naithani, S., Khullar, R., Bhatt, A. and Soni, P.L., 2006. Carboxymethylation of α-cellulose isolated from Lantana camara with respect to degree of substitution and rheological behavior. *Carbohydrate Polymers*, *63*(1), pp.40-45.

Vernon-Parry, K.D., 2000. Scanning electron microscopy: an introduction. *III-Vs Review*, *13*(4), pp.40-44.

Wang, Y., Zhang, C., Zhao, L., Meng, G., Wu, J. and Liu, Z., 2017. Cellulose-based porous adsorbents with high capacity for methylene blue adsorption from aqueous solutions. *Fibers and Polymers*, *18*(5), pp.891-899.

WHD Microanalysis consultants., 2017. SEM Introduction: An Overview of Scanning Electron Microscopy. Available: https://www.understanding-cement.com/sem-introduction.html (Accessed January 2018)

Wilson, R., 2013. Challenges pulp and paper producers face entering new markets. *Appita Journal: Journal of the Technical Association of the Australian and New Zealand Pulp and Paper Industry*, *66*(3), p.170.

Xiros, C. and Christakopoulos, P., 2012. Biotechnological potential of brewers spent grain and its recent applications. *Waste and Biomass Valorization*, *3*(2), pp.213-232.

Yang, H., Yan, R., Chen, H., Lee, D.H. and Zheng, C., 2007. Characteristics of hemicellulose, cellulose and lignin pyrolysis. *Fuel*, *86*(12-13), pp.1781-1788.

Yaşar, F., Toğrul, H. and Arslan, N., 2007. Flow properties of cellulose and carboxymethyl cellulose from orange peel. *Journal of Food Engineering*, *81*(1), pp.187-199.

Yu, M., Han, Y., Li, J. and Wang, L., 2017. One-step synthesis of sodium carboxymethyl cellulose-derived carbon aerogel/nickel oxide composites for energy storage. *Chemical Engineering Journal*, *324*, pp.287-295.

Zafar, S. (2015). Energy potential of bagasse. BioEnergy consultant. (https://www.bioenergyconsult.com/tag/what-is-bagasse/ Accessed June 2016)

ZF Biochemical., 2017. CMC Tobacco grade. Available: http://www.zf-biochemical.com/e_productshow/?28-Carboxyl-Methyl-CelluloseCMC-CMC-tobacco-grade-28.html (Accessed 2017).

Zhang, G., Zhang, L., Deng, H. and Sun, P., 2011. Preparation and characterization of sodium carboxymethyl cellulose from cotton stalk using microwave heating. *Journal of Chemical Technology & Biotechnology*, *86*(4), pp.584-589.

Zimmermann, T., Pöhler, E. and Schwaller, P., 2005. Mechanical and morphological properties of cellulose fibril reinforced nanocomposites. *Advanced Engineering Materials*, *7*(12), pp.1156-1161.